

Mediterranean Marine Science

Vol 16, No 2 (2015)



Biological response to geochemical and hydrological processes in a shallow submarine cave

M. RADOLOVIĆ, T. BAKRAN-PETRICIOLI, D. PETRICIOLI, M. SURIĆ, D. PERICA

doi: [10.12681/mms.1146](https://doi.org/10.12681/mms.1146)

To cite this article:

RADOLOVIĆ, M., BAKRAN-PETRICIOLI, T., PETRICIOLI, D., SURIĆ, M., & PERICA, D. (2015). Biological response to geochemical and hydrological processes in a shallow submarine cave. *Mediterranean Marine Science*, 16(2), 305–324. <https://doi.org/10.12681/mms.1146>

Biological response to geochemical and hydrological processes in a shallow submarine cave

M. RADOLOVIĆ¹, T. BAKRAN-PETRICIOLI¹, D. PETRICIOLI², M. SURIĆ³ and D. PERICA⁴

¹ University of Zagreb, Faculty of Science, Department of Biology, Rooseveltov trg 6, 10000 Zagreb, Croatia

² D.I.I.V. Ltd., for marine, freshwater and subterranean ecology, 23281 Sali, Croatia

³ University of Zadar, Department of Geography, Ulica dr. Franje Tuđmana 24i, 23000 Zadar, Croatia

⁴ University of Zadar, Department of Geography, Trg kneza Višeslava 9, 23000 Zadar, Croatia

Corresponding author: tatjana.bakran-petricioli@zg.t-com.hr

Handling Editor: Carlo Bianchi

Received: 24 November 2014; Accepted: 5 January 2015; Published on line: 27 April 2015.

Abstract

The Croatian coastal karst abounds in submerged caves that host a variety of environmental conditions depending on the geomorphology, depth and submarine groundwater discharge. One example is the Y-Cave, a shallow, mostly submerged, horizontal cave on Dugi Otok Island, on the eastern Adriatic coast. This study was aimed at examining the temporal and spatial variability of the marine cave environment, including temperature, salinity, light intensity, cave morphology and hydrodynamism, along with the dissolutional effect caused by the mixing of sea and freshwater. The general distribution of organisms in the Y-Cave was positively correlated to the light gradient and reduced water circulation, thus the highest species diversity and abundance were recorded in the front part of the cave. The phylum Porifera was the most dominant group, and the poriferan species diversity in the cave ranks among the ten highest in the Mediterranean. The middle part of the cave, although completely dark, hosts an abundant population of the gastropod *Homalopoma sanguineum* and clusters of the gregarious brachiopod *Novocrania anomala*, whose presence could be connected to tidal hydrodynamics. The absence/scarcity of sessile marine organisms and pronounced corrosion marks at shallow depths inside the cave suggest a freshwater impact in the upper layers of the water column. A year long experiment with carbonate tablets revealed three different, independent ongoing processes affected by the position in the cave: bioaccumulation, dissolution and mechanical erosion. The results of long-term temperature readings also revealed water column stratification within the cave, which was not disturbed by either tidal or wave action. The shallow, partly submerged and relatively small Y-Cave is characterised by a suite of complex environmental conditions, which, together with the resulting distribution of organisms, are unique to this cave.

Keywords: Submerged cave, karst, mixing corrosion, biodiversity, Porifera, Adriatic Sea.

Introduction

Caves are natural underground voids usually formed in karst. They exhibit a unique environment generally characterized by stable environmental conditions throughout the year – primarily air temperature (equivalent to the mean annual surface atmosphere temperature) and relative humidity (approaching 100%). They are oligotrophic, aphotic subterranean habitats inhabited by scarce cave biota adapted to reduced light and near-constant temperature regimes, and are dependent on periodic inputs of food, usually swept in by floods (Gillieson, 1996). Once drowned by the rising sea, submerged caves within the marine environment also host relatively stable conditions regarding temperature and water chemistry. Throughout the transition of the cave from completely subaerial to an entirely marine environment, extreme conditions occur due to the interaction of different geochemical and hydrogeological settings. In particular, in the coastal zone, groundwater and sea levels oscillate in near synchrony, so as sea-levels rise, coastal caves expe-

rience a transition through vadose, littoral, anchialine and (sub)marine conditions (Surić *et al.*, 2005; Van Hengstum *et al.*, 2011). One of the most pronounced geochemical effects is produced by the interaction of fresh water and sea water, known as mixing corrosion (introduced as *Mischungkorosion* by Bögli (1964)). The mixing of two solutions saturated at different partial pressures of CO₂ yields a third solution that is undersaturated with respect to calcite (Frank *et al.*, 1998; Kaufmann & Dreybrodt, 2007) (Fig. 1). After a relatively long time underground, groundwater (H₂O-CO₂-CaCO₃ solution) that percolates within the epikarst and emerges in the cave is commonly supersaturated with respect to calcite (Fairchild & Baker, 2012), enabling the precipitation of speleothems. Sea water is also supersaturated with CaCO₃ down to the first 500 m (Kennett, 1982), enabling marine organisms to build their shells. The mixing of these two waters takes place in the coastal zone at the interface where denser sea water intrudes into the karst aquifer as a wedge under a fresh groundwater lens, and it is responsible for the dis-

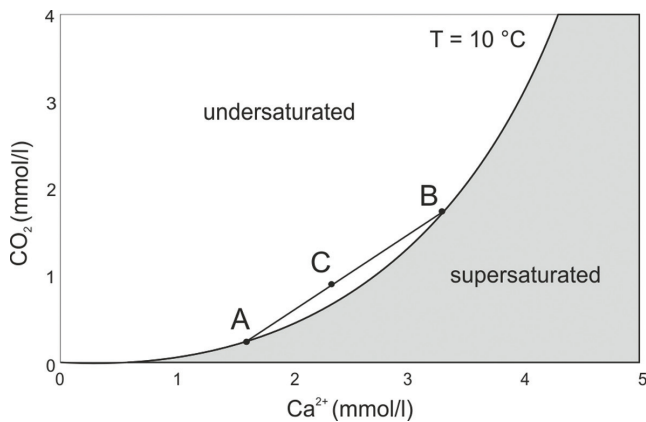


Fig. 1: The non-linear relationship between CO_2 and Ca^{2+} concentrations in $\text{H}_2\text{O}-\text{CO}_2-\text{CaCO}_3$ solution. Each mixture (e.g. C) of the saturated solutions A and B lies on the straight line between them in the zone of undersaturation with respect to calcite, producing an aggressive solution that dissolves the surrounding carbonate (after Gabrovšek & Dreybrodt (2010)).

solutional effects that influence carbonate in caves within the mixing zone, regardless of whether it is primary limestone bedrock, secondary deposited flowstone or organogenic carbonate produced by marine organisms.

As dissolution is one of the main processes of karstification, different methods have been used in order to assess its temporal and spatial dimensions, as outlined in Gabrovšek (2009). One such method is the weight loss measurements of “standard” limestone tablets exposed to dissolution in different environments, though the very few data published have exclusively regarded dissolution in continental environments (Gams, 1985; Plan, 2005; Zhang, 2011; Buzjak *et al.*, 2013; Krklec *et al.*, 2013 and references therein). Dissolution at the groundwater-seawater interface has not previously been recorded using the method of limestone tablets, despite the suggestion that dissolution may be a principal mechanism of cave and karst development in the coastal zone (Myroie & Myroie, 2007). With more than 235 known submerged caves (Surić *et al.*, 2010), and thousands likely yet to be explored, the Croatian submerged karst offers exceptional potential for such studies.

From the biological point of view, the variety of coastal and marine geomorphic features offers a great diversity of submerged karst habitats (Bakran-Petricioli & Petricioli, 2008), such as completely or partially submerged pits, caves and submarine passages. Marine caves have unique faunistic and ecological characteristics, and the organisms and communities inhabiting them exhibit distinctive zonation (Pérès & Picard, 1964; Riedl, 1966; Harmelin *et al.*, 1985; Bianchi & Morri, 1994; Bianchi, *et al.* 1996; Harmelin, 1997). The decreasing species richness, abundance and biomass from the entrance towards the end of marine caves is explained by a gradient of environmental factors, primarily the attenuation of light and hydrodynamics (Riedl, 1966; Cinelli *et*

al., 1977; Harmelin *et al.*, 1985; Gili *et al.*, 1986; Balduzzi *et al.*, 1989; Rosso *et al.*, 2012). However, a study by Zabala *et al.* (1989) showed in an examined cave in the Western Mediterranean that zonation cannot be explained simply with a decrease in water motion and food supply. Moscatello & Belmonte (2007) also noted that although the innermost portion of a cave in the southern Adriatic showed benthic faunal depletion, a rich presence of plankton was recorded there. Recent studies using stable isotope signatures to investigate cave mysid feeding strategies have shed more light on resource partitioning in marine caves (Rastorgueff *et al.*, 2011).

Classically, two distinctive biocoenoses could be recognized within marine caves (Pérès & Picard, 1964): the biocoenosis of semi-dark caves (*biocoenose des grottes semi-obscurées*, GSO) and the biocoenosis of caves and ducts in total darkness (*biocoenose des grottes et boyaux à obscurité totale*, GO). GSO is located near the cave entrances and is characterized by high species diversity and biomass, dominated by massive sponges, cnidarians (class Anthozoa) and branched bryozoans. GO occupies the innermost parts of the caves, where the biodiversity and biomass are much lower, and the fauna is characterized by encrusting sponges, bryozoans and sessile polychaetes. In the latter biocoenosis, rocks are usually barren and blackened by iron and manganese oxides of bacterial origin. Completely dark caves, especially those that trap cold seawater, can be considered extensions of the bathyal zone. They are often inhabited by deep sea organisms and are thus very interesting scientifically (Harmelin *et al.*, 1985; Vacelet *et al.*, 1994; Bakran-Petricioli *et al.*, 2007; Janssen *et al.*, 2013).

Different studies have shown that within caves there are transitions between the biocoenoses of semi-dark and dark caves. Laborel & Vacelet (1959) described a transition zone between GSO and GO where sponges and stony corals are still present, though species more characteristic for GSO begin to disappear, and species specific to GO begin to appear. Harmelin *et al.* (1985) described a transition zone between the two biocoenoses, which is dominated by bryozoan nodules. Similar structures have been found in other caves (Rosso *et al.*, 2013).

A spatial variation in benthic assemblages was recorded in the span of a few meters within a marine cave (Benedetti-Cecchi *et al.*, 1996). The study of two caves in the north-western Mediterranean revealed that the distinct morphology of the cave, *i.e.* its depth and geographic location, actually influence water movement, food availability and light penetration, and their interplay causes differences in the communities (Martí *et al.*, 2004). Inconsistent spatial and temporal changes in assemblages, as a result of multiple and interactive ecological processes, were also recorded in three shallow marine caves in southern Italy (Bussotti *et al.*, 2006).

Marine caves are recognized as habitats important for conservation. They have been included in the Habi-

tats Directive of the European Union (Council Directive 92/43/EEC) and are also protected in Croatia (Bakran-Petricioli, 2011). Their poor resilience and vulnerability to different disturbances from diving to climate change has already been well documented (Chevaldonné & Lejeusne, 2003; Parravicini *et al.*, 2010; Guarnieri *et al.*, 2012; Giakoumi *et al.*, 2013).

This study provides a report of the settings where hydrologically and geomorphologically induced geochemical features significantly influence biological distribution in the Y-Cave, a shallow coastal cave partially submerged by sea water on the eastern Adriatic coast. The aim of this study was to determine the distribution of benthic organisms and communities along the cave conduits in relation to cave morphology, temperature, light intensity, hydrodynamics and geochemical settings, and to assess how the dissolutional effect in the mixing zone influences not only biological components, but also the cave environment as a whole.

Study area and environmental settings

The eastern Adriatic coast is part of the Dinaric *Classical karst* formed within the up to 8 km thick succession of shallow-water carbonate sediments deposited mostly during the Mesozoic and the Paleogene (Vlahović *et al.*, 2005). The emersion of the carbonate bedrock along with

intensive folding and faulting generated by the Alpine orogeny was followed by overall karstification. A vast part of that karstified area was subsequently submerged by the last late Pleistocene–Holocene sea transgression, transforming originally subaerial karst features (karrens, dolines, karstic springs, etc.) into submarine ones, including numerous caves (Pikelj & Juračić, 2013). Presently, of more than 235 known submerged caves, more than half are completely marine (euhaline), whilst environmental conditions in others (mainly coastal caves) vary depending on depth, tide and seaward freshwater discharge (Surić *et al.*, 2010). One such cave is the Y-Cave ($44^{\circ}03'27.3''$ N; $14^{\circ}59'04.8''$ E), located in the central Adriatic on the south-western coast of Dugi Otok Island near Brbišćica Cove (Fig. 2), with the entrance at 12 m below the mean sea level (Juračić *et al.*, 2002). It is a shallow, almost completely submerged cave, except one small chamber with an air pocket (profile C-C' in Fig. 2) developed above the junction of the two main channels. The cave is formed in well-bedded Upper Cretaceous (Turonian) fossiliferous limestone (Fuček *et al.*, 1991), and its speleogenesis and simple morphology was predetermined by tectonics, i.e. two fissures striking $0-180^{\circ}$ and $64-244^{\circ}$ that were subsequently enlarged by groundwater flow. In a later phase of speleogenesis, speleothems were precipitated, and finally, the late Pleis-

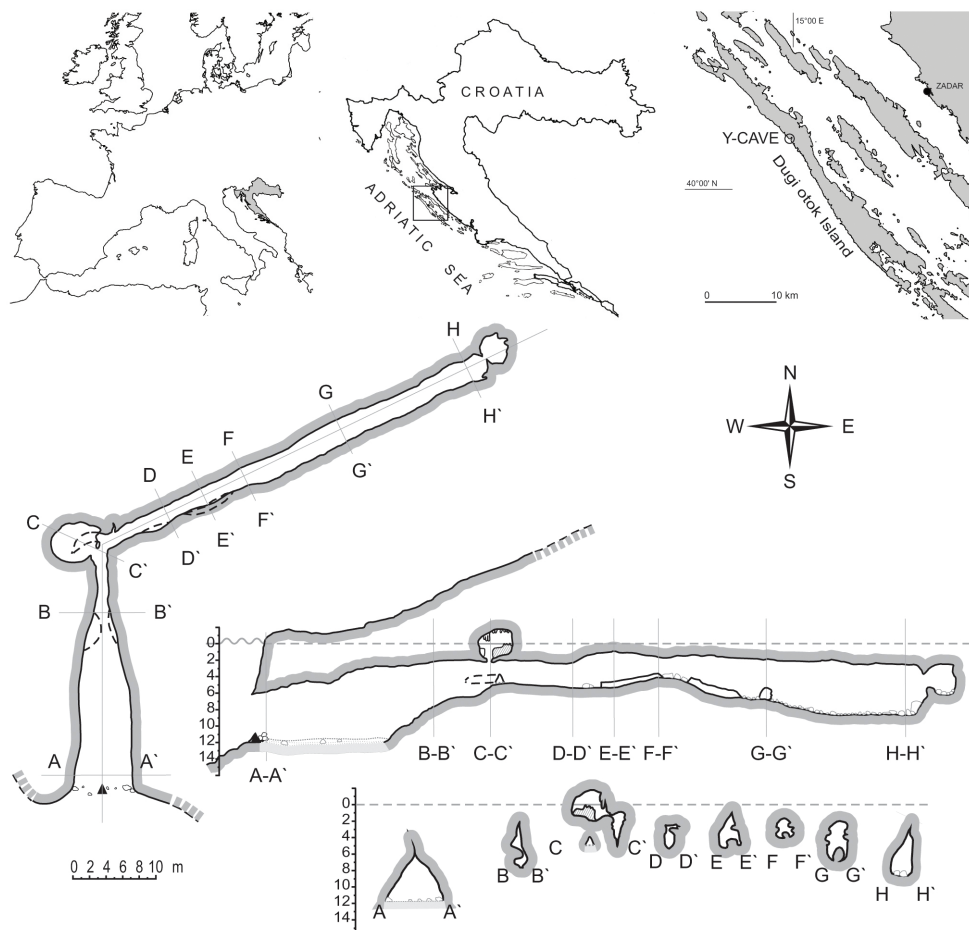


Fig. 2: The location, cross-section and layout of the Y-Cave on Dugi Otok Island, Croatia, with characteristic profiles.

tocene–Holocene sea-level rise partially submerged the Y-Cave, along with several other similar features in the surroundings of Brbišćica Cove.

The intensive karstification of the carbonate bedrock of Dugi Otok Island resulted in the absence of surface runoff and a fast, direct infiltration of meteoric water into the underground. Infiltration is discrete and occurs through open fractures, leading to a relatively short mean residence time of groundwater in the karst underground (Terzić *et al.*, 2007). Due to the shape of the island (45 km long and only 2 km wide in places; total surface of 114.44 km²) (Fig. 2), it is unrealistic to expect a large groundwater body. Unlike the northern part of the island (Terzić *et al.*, 2007), the aquifer near the Y-Cave is not protected from sea intrusion, and normal groundwater-seawater contact of the unconfined coastal karst aquifer can be expected. In a coastal cave, this is marked by a thin freshwater lens overlying the seawater wedge that intrudes into the aquifer under the freshwater (Terzić *et al.*, 2010). Such submarine groundwater discharge (SGD) usually has significant biogeochemical importance through the provision to nutrients to specialized coastal habitats (Bokuniewicz *et al.*, 2003; Burnett *et al.*, 2003; Sanfilippo *et al.*, 2014), as in the case of the Y-Cave.

Although the Adriatic is a landlocked sea, it is influenced by dynamic meteorological conditions (Cushman-Roisin *et al.*, 2001). The south-eastern wind (sirocco) with a sufficiently long wind fetch can generate waves with a maximum recorded height of 10.8 m (Leder *et al.*, 1998). Yet, the highest wave impact on the south-western coasts is generated when the waves produced by the SE wind sirocco interfere with those of the S wind (ostro) or SW wind (libeccio), during a change of the synoptical situation above the Adriatic Sea, primarily during winter. Given the location of the Y-Cave on the SW coast of the island facing the open sea (Fig. 2), relatively high wave energy can be expected.

Generally, a mixed semidiurnal tide type prevails in the Adriatic Sea, although the tide maintains a diurnal character in proximity of the semidiurnal amphidromic point which is positioned on the Ancona - Šibenik line (Lovato *et al.*, 2010), which is in relatively proximity to the Y-Cave. The tidal range from the adjacent Zadar tide gauge is 29 cm (HHI, 2012). The interaction of all these geological, geomorphic, hydrogeological, meteorological and oceanological properties, along with site-specific light intensity and temperature settings, produces a spectrum of different habitats populated by characteristic marine biocoenoses.

Materials and Methods

The first phase of the Y-Cave research (2003–2006) encompassed detailed cave mapping of underground conduits and cavities using standard topographical/speleological surveying techniques, and biological mapping by numerous SCUBA speleo-dives. In order to protect

the cave biota, most of the species were noted and determined *in situ*, and others were sampled and preserved in a 96% solution of ethyl alcohol for subsequent determination in the laboratory. Sampling was performed in the least destructive manner possible, *i.e.* only problematic species or species unable to be determined *in situ* were sampled. Therefore, the relative abundance of species was estimated rather than determined quantitatively. Sponges were identified using light microscopy of skeletal characters according to the current taxonomic literature. When necessary, for higher taxonomic categories, Systema Porifera (Hooper & Van Soest, 2002) was consulted. For corals and bryozoans hydrogen peroxide (H₂O₂ conc. 6%) or sodium hypochlorite (NaOCl conc. 6%) were used for the degradation of organic matter. The scientific names are listed according to the European Register of Marine Species (Costello *et al.*, 2014) and the World Porifera database (Van Soest *et al.*, 2014).

For photo documentation, two underwater cameras were used: analogue Nikonos V and Canon A75 with an underwater case. The photos from the Nikonos V were digitalised and all photos were analysed in order to obtain additional data and to complement the list of species (Appendix, Table 2).

A simple species diversity index, Sorensen's Quotient of Similarity ($Q/S=2j/(a+b)*100$; where a is the total number of species in one part of the cave, b is the total number of species in the other part of the cave and j is the number of species common to both parts), was calculated for the front, middle and end part of the Y-Cave.

In order to estimate the environmental conditions that govern the distribution of marine organisms, thermohaline properties and light intensity were measured at specific sites along the cave channel. Water temperature was measured with small stow away temperature data loggers (Onset Computers®, ±0.2°C accuracy) with a set sampling interval of 16 min. The loggers were placed at selected positions and depths in the cave as shown in Figure 3 and Table 1. The measurement started on August 27, 2003 and ended on July 4, 2004 (for loggers 2, 4, 6) and on October 8, 2004 (for loggers 1, 3, 5).

Light intensity was measured during eleven days using Onset Computers® light data loggers that were set at ten positions along the cave (Fig. 3). In four light data loggers, the photosensitive cell was facing upwards (data loggers with a black dot in Fig. 3) while in the remaining six loggers, the cell was positioned to face the entrance of the cave. In the entrance part of the cave, three pairs of loggers (2 & 3, 4 & 5, 6 & 7) with different sensor cell orientations were set to determine whether the position of the photosensitive cell affects the measurement. Light intensity was recorded every two minutes during the period from June 19 to 30, 2006.

Thermohaline properties of the water column inside the Y-Cave were measured with the Idronaut® Ocean Seven 316 CTD probe on August 27, 2003. The probe

Table 1. Mass difference (Δm) of the limestone tablets and dissolution rate (R) at 6 different positions within the Y-Cave after the 1-year exposure period. Measurement positions are marked on Figure 3. Note that positive values indicate dissolution, while negative values indicate the increase of the tablet mass.

Measurement site	Location within the cave	Depth (m)	$\Delta m = m_{\text{init}} - m_{\text{fin}}$ (g)	R ($\mu\text{g/a}$)
1	Entrance of the cave - bottom	11.5	-0.2051	-20.9750
			-0.2207	-22.5703
			-0.1453	-14.8594
2	Middle portion of the entrance part - ceiling	2.9	-0.0036	-0.3682
			-0.0028	-0.2863
			0.0011	0.1125
3	Chamber with air pocket and speleothems	0.7	0.0022	0.2250
			0.0008	0.0818
			0.0054	0.5522
4	Central portion of the cave - bottom	5.1	-0.0068	-0.6954
			-0.0047	-0.4807
			0.0173	1.7692
5	End of the cave - ceiling	3.9	-0.0054	-0.5522
			-0.0095	-0.9715
			-0.0026	-0.2659
6	End of the cave - bottom	8.5	0.007	0.7159
			0.0333	3.4055
			0.2013	20.5863

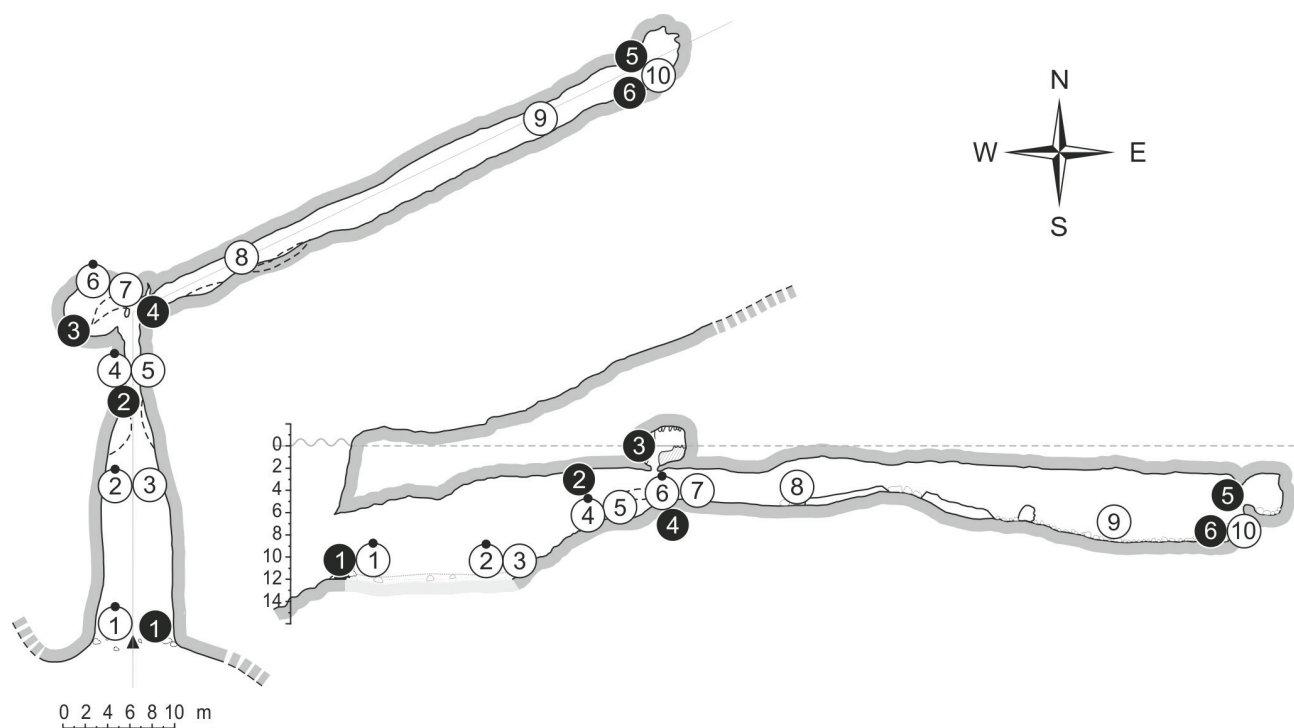


Fig. 3: The positions of temperature and light intensity data loggers inside the Y-Cave (dark circles - temperature data loggers; white circles - light intensity data loggers). Four loggers with their photosensitive cell facing upwards are marked with a black dot; the remaining cells were positioned to face the entrance of the cave.

was programmed to record data every two seconds. The data was processed with the REDAS® (Real Time Data Acquisition Software). The diver (D. Petricoli) carried the probe along the cave and made six vertical profiles with it at specific locations, carefully lowering the probe from the ceiling towards the bottom. Vertical profile no. 1 was performed at the cave entrance from the water sur-

face down to 12.5 m depth; profile no. 2 was performed inside the cave entrance from 2 to 12 m depth; profile no. 3 was performed at the turning point (junction of two main channels), approximately at section C-C'; vertical profiles no. 4 to 6 were performed in the inner part of the cave: no. 4 approximately at section E-E', no. 5 approximately at section G-G' and no. 6 approximately at section

H-H' (see Fig. 2 for the position of the sections). An additional vertical profile was performed from the surface down to 29 m depth in front of the cave.

Behind the B-B' cross-section (Fig. 2), at 5.5 m depth, an unusual pink coloured, coarse sediment was sampled. The sample was fixed in 96% ethyl alcohol and further separated in the laboratory into four categories combining two criteria: origin (terrigenous/organogenic) and size (diameter less than/greater than 4 mm). The shells of the marine gastropod *Homalopoma sanguineum* were also separated due to their unusually high abundance. The mass and volume fractions of each category were determined after drying (70°C for 3 days).

In order to assess the carbonate dissolutional effect within different submerged parts of the cave, sets of limestone tablets (coupled with temperature loggers) were positioned and left exposed for more than one year (from August 27, 2003 to October 8, 2004) at six distinct sites as shown in Figure 3. The tablets were made of a borehole core of Cretaceous (Senonian) limestone from a quarry near Lipica (Karst plateau, Slovenia), and measured 41.1 mm in diameter and 3–5 mm in thickness. Four holes, 3 mm in diameter, were drilled in each tablet for fixation in the field. The tablets were precisely pre-weighted and tied in series of three for each measuring point. After the 1-year exposure to the biogeochemical and hydrodynamic influence of groundwater and/or seawater, the changes in tablet mass were again precisely measured. Dissolution rates were calculated following the expression (1) (after Plan, 2005 modified by Buzjak *et al.*, 2013):

$$R = \frac{(m_{\text{init}} - m_{\text{fin}})}{A \times \rho} \times \frac{365}{t} \quad (1)$$

where R is the dissolution rate ($\mu\text{m/a}$); $(m_{\text{init}} - m_{\text{fin}})$ is the mass difference (g); ρ is the limestone density (2.68 g/cm^3), t is the time span (408 days) and A is the area of the initial soluble surface (32.64 cm^2). The exposed surface A (cm^2) was calculated using the expression (2) taking into consideration the surface of the tablet and of the four holes:

$$A = 2r_1\pi(H+r_1) + 8r_2\pi(H-r_2) \quad (2)$$

where r_1 is the radius of the tablet (cm), r_2 is the radius of the hole (cm) and H is the thickness of the tablet (cm). The dissolution rate unit $\mu\text{m/a}$ (mm/ka) is the most common, and can be read as $\text{m}^3/\text{km}^2/\text{a}$ (Plan, 2005) when it stands for the denudation rate.

Results

Marine organisms and communities

Within the Y-Cave, two typical marine cave biocoenoses were identified. A well-developed GSO (Fig. 4, A-E) with high species diversity and biomass dominated from the entrance to approximately section C-C' (Fig. 2). The GO with low species diversity and biomass, is present deeper in the cave (Fig. 4, H), approximately

from the section E-E' to the end of the cave. The middle portion of the cave could be characterized as a transition from GSO to GO (Fig. 4, F-G).

In total, 139 taxa of marine organisms were recorded in the Y-Cave, among which sponges dominated with 56 taxa (Appendix, Table 1). Three classes of this phylum were recorded: Calcarea (6 taxa), Demospongiae (47 species) and Homoscleromorpha (3 species). Among the 83 taxa of other organisms, 5 algal species were recorded (only in the entrance part; Chlorophyta 2 and Rhodophyta 3), 1 benthic foraminifer, 9 species of cnidarians (all belonging to Anthozoa), 1 echinuran species, 23 mollusc taxa (15 gastropods, 7 bivalves and 1 cephalopod), 4 polychaete taxa, 6 crustacean species, 7 bryozoan species, 2 brachiopod species, 9 echinoderm species, 1 ascidian species, and 15 fish species. The majority of taxa (122) were observed in the front part of the cave, while 42 taxa were noted in the middle part of the cave (section C-C' to approximately section E-E'), and only 20 species were noted in the innermost part (from section E-E' towards the end of the cave). Furthermore, 93 taxa were noted only in the front part of the cave, 6 only in the middle part and 4 only in the end part. Also, 20 taxa were found in both the front and the middle part of the cave and 7 in the middle and the end part of the cave, while 9 sponge species were present throughout the cave with decreasing abundance and body size towards the end (Appendix, Table 1). Of these, *Chondrosia reniformis* and *Petrosia (Petrosia) ficiformis* were completely white inside the cave due to the lack of light and therefore the absence of endosymbiotic algae that give them their characteristic colouration (Fig. 4 E). In the middle and end parts of the cave, virtually no sessile marine organisms were noted on walls shallower than 2 m depth (Fig. 11).

The end part of the cave was characterized by low species richness and low relative abundance and by distinct faunal depletion (Fig. 4 H; Appendix, Table 2) that is typical for GO. Barren rock was easily seen and the fauna consisted of scarce populations of small and/or encrusting forms of demosponges and homoscleromorphs, small calcareous sponges, and small serpulids.

Three sponge species with cave affinities characterize the inner dark part of the Y-Cave: *Discodermia polymorpha* (rare), *Myrmekioderma spelaenum* (common) and *Placospongia decorticans* (common; Fig. 4 G). Other common sponge species inside the dark part of the cave were: calcareous *Amphoriscus chrysalis*, *Sycon elegans* and *Sycon* sp., demosponges *Chondrosia reniformis*, *Cliona schmidtii*, *Diplastrella bistellata*, *Petrosia (Petrosia) ficiformis*, *Spirastrella cunctatrix*, *Spongia (Spongia) virgultosa*, and homoscleromorphs *Corticium candelabrum* and *Plakina bowerbanki*. None of these species showed any particular dominance in respect to the others.

In terms of species diversity, the middle and end parts of the cave were the most similar (50.0% of similarity), the front and middle parts were less similar (35.4%) and the front and

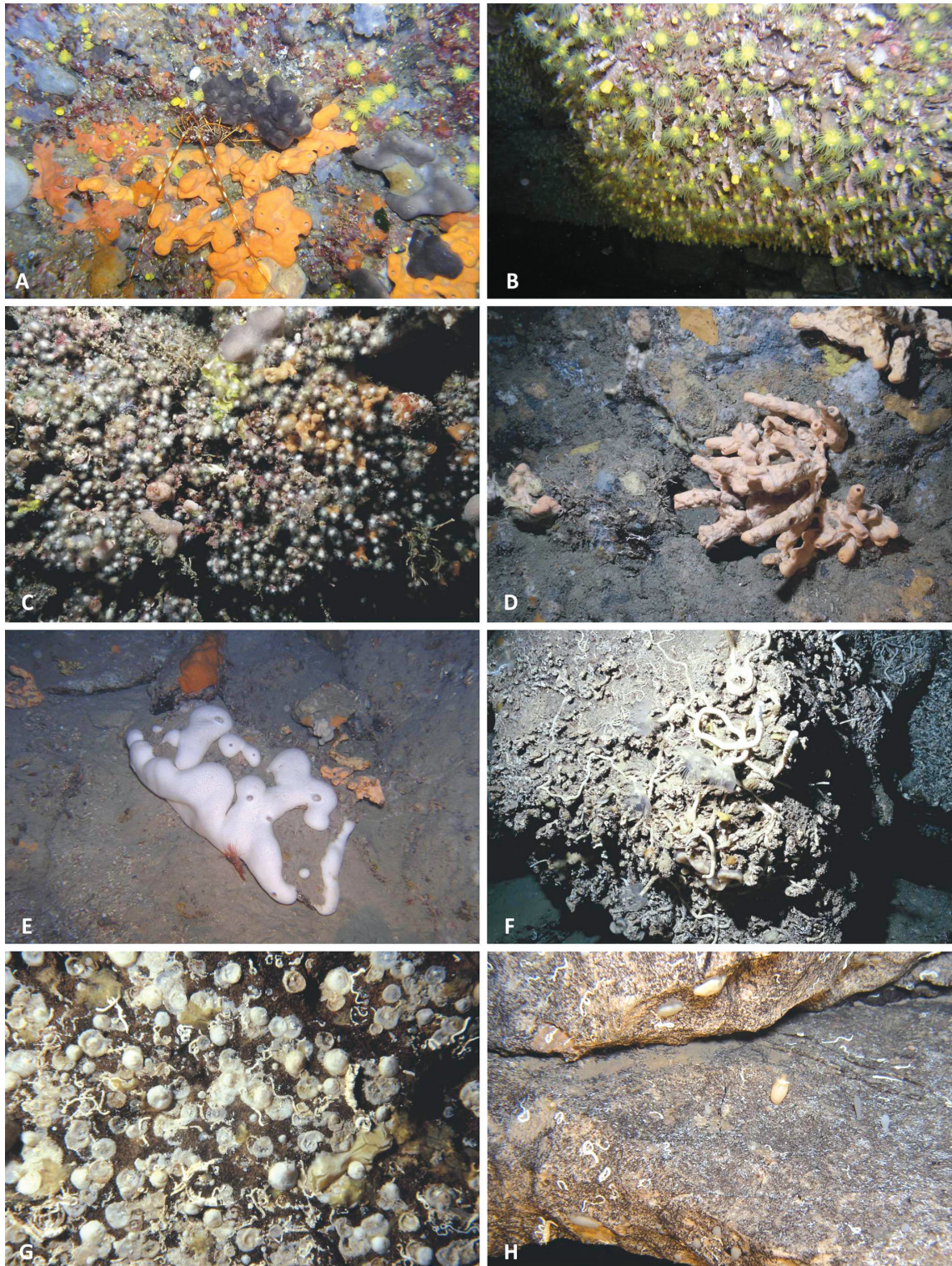


Fig. 4: Living communities inside the Y-Cave: A) the entrance part of the cave, vertical wall, depth 9 m, biocenosis of semi-dark caves (GSO, see text for explanation of acronym) dominated by numerous sponge species; B) the entrance part of the cave, ceiling, depth 6 m, GSO dominated by scleractinian coral *Leptopsammia pruvoti*; C) the entrance part of the cave, overhang, depth 7 m, GSO dominated by scleractinian coral *Madracis pharensis*; D) the entrance part of the cave, vertical wall (near the bottom), depth 9 m, GSO, a large specimen of the orange sponge *Agelas oroides* dominates the photo; E) the middle part of the cave, in front of the section C-C', bottom, depth 10 m, a massive white specimen of the sponge *Chondrosia reniformis*; F) the middle part of the cave, between sections C-C' and D-D', vertical wall and overhang, depth 5 m, the transition from GSO to biocenosis of caves and ducts in total darkness (GO, see text for explanation of acronym), the community is dominated by serpulids; G) the middle part of the cave, between sections C-C' and D-D', vertical wall, depth 5 m, transition from GSO to GO, a dense population of brachiopod *Novocrania anomala*, encrusting sponge *Placospongia decorticans* and serpulids; H) the end part of the cave, near the section G-G', vertical wall with overhang and horizontal shelf, depth 6 m, GO with scarce calcareous sponges and serpulids (see Fig. 2 for position of the sections).

end parts of the cave were the least similar (12.7%).

Within the Y-Cave, 15 fish species were noted, virtually all in the front part of the cave (14 of 15; Appendix, Table 2). The only fish species recorded at the end part of the cave was the speleophilic species *Grammonus ater*. Only two species could be considered common inside the cave: *Apogon imberbis* and the speleophilic *Thorogobius ephippiatus* and they were noted in the front and middle parts of the cave.

Temperature, salinity and light intensity

The annual variations of water temperature in the entrance part of the cave and at five positions inside the cave are shown in Figure 5. Temperature readings revealed a complex seasonal distribution of water layers in the cave from August 2003 to July/October 2004: the retention of warm water (>15°C) in the shallower parts of the cave during winter (loggers 2, 3 and 5), the existence and retention of a cold water (18–22°C) layer inside the chamber with speleothems and air pocket during summer 2004 (logger 3), the retention of colder water in deeper parts inside the cave throughout the year (logger 6), and rapid periodical changes of water temperature in the mid-

dle part of the cave during winter (logger 4).

Since there was a prominent winter temperature fluctuation recorded by logger 4 (Fig. 5) at a depth of 5.1 m in the middle part of the cave, this was compared to the tide records of the nearest tide gauge at the port of Zadar for the period from February 2–8, 2004. Figure 6 clearly shows inverse fluctuations, i.e. a temperature increase of approximately 3°C with each low tide, and a drop with each high tide.

Vertical temperature profiles outside, at the entrance, and inside the Y-Cave, taken with the CTD probe in summer 2003, revealed that the thermocline outside the cave and in the entrance part was at around 10 m depth, which is approximately 5 m deeper than in the inner part of the cave (Fig. 7). At the end part of the cave (at sections G-G' and H-H'; Fig. 2) the thermocline was at around 5 m and a sudden temperature drop of 7°C occurred within one meter depth.

Vertical temperature and salinity profiles recorded with the CTD probe during the dive inside the Y-Cave on August 27, 2003 are presented in Figure 8. At the time of recording, the salinity throughout the cave showed a fully marine environment. Although salinity oscillations were minimal, approximately 1 PSU, it was notable that in all vertical profiles, except for profile no. 3, salinity rose slightly with each dive.

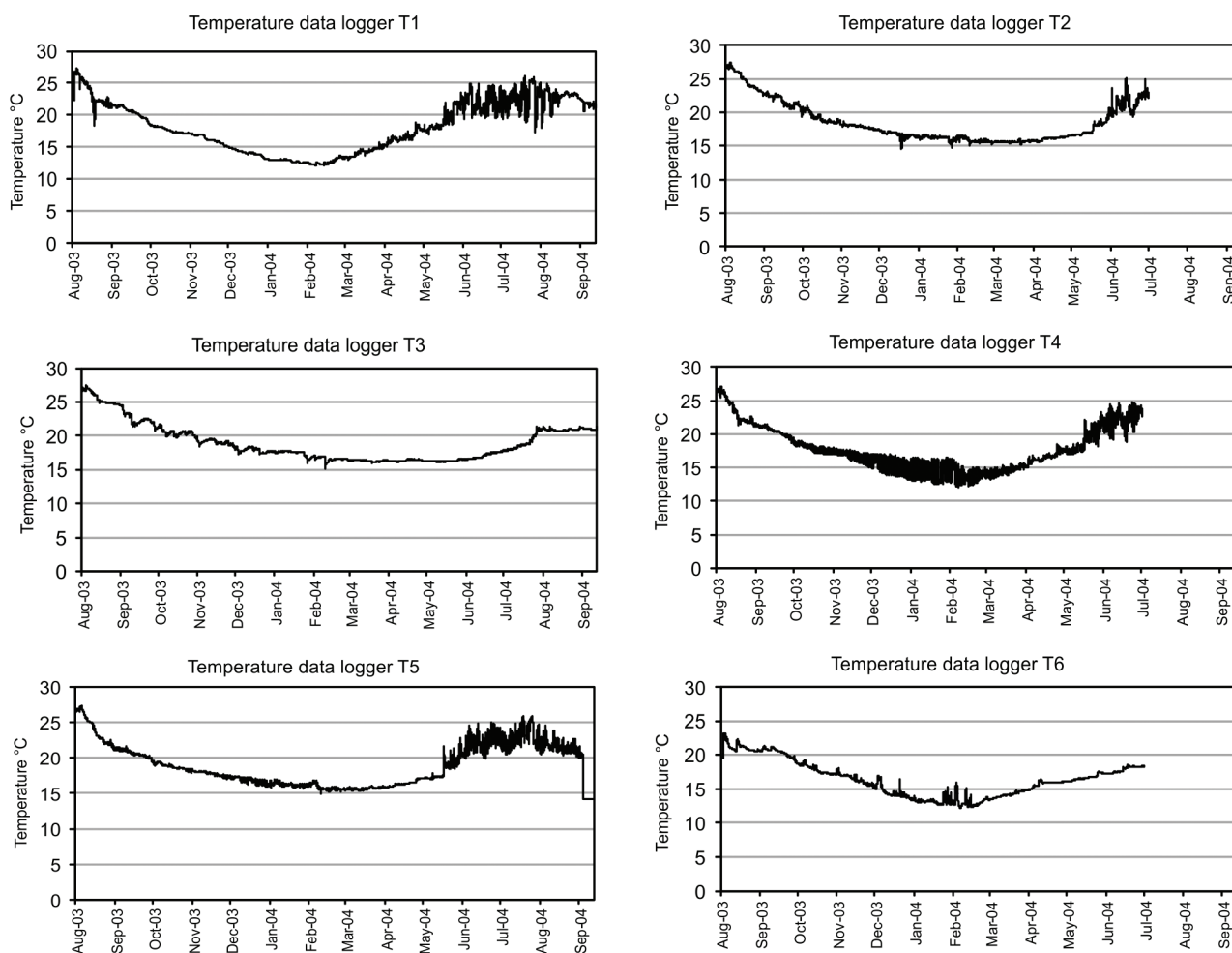


Fig. 5: The annual variation of temperature along the Y-Cave (from August 23–27, 2003 to July 4/October 8, 2004). Measurement positions are given in Fig. 3 and depths in Table 1.

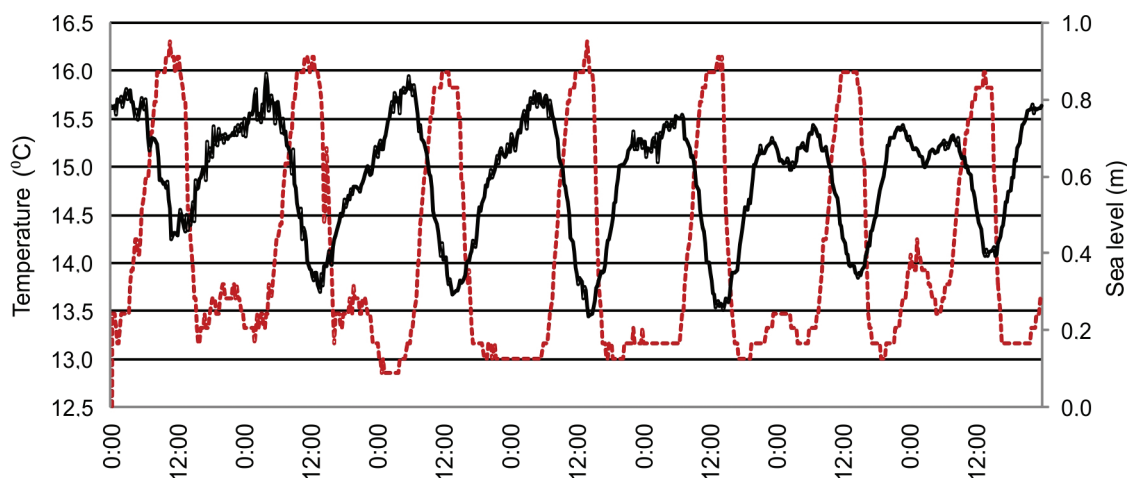


Fig. 6: The comparison of the tidal (solid line) and temperature (dashed line) fluctuation from February 2–8, 2004. Temperature records are from logger 4 (Fig. 3), and tides from the nearest tide gauge in Zadar port.

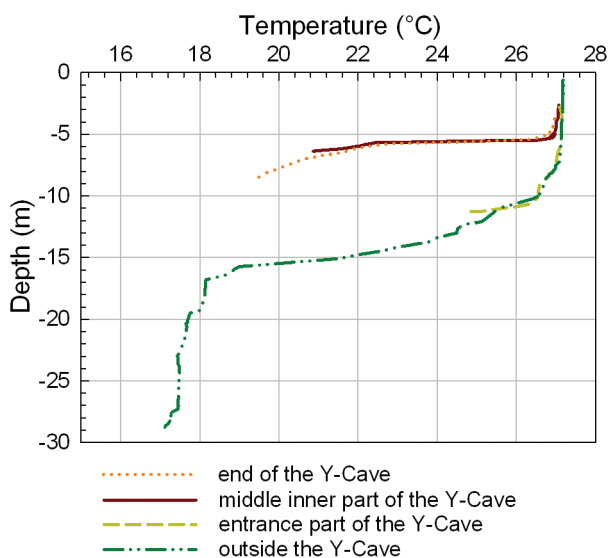


Fig. 7: Vertical temperature profiles inside and outside the Y-Cave taken with the CTD probe (August 27, 2003); the profile labelled with a dotted line was taken at approximately section H-H', the profile labelled with a solid line at approximately section G-G'.

The light intensity measurement taken over a period of 11 days in June 2006 showed that the orientation of the photosensitive cell did not yield any prominent differences in the measurement, and that virtually no light penetrated into the cave after logger 4 (see position in Fig. 3). Figure 9 shows the results of the light intensity measurements at only the most representative positions, i.e. logger 1 at the entrance, logger 4 in the middle part and logger 10 at the end part of the cave.

Cave sediment

The mass and volume fractions of four sediment categories in the coarse sediment sample collected behind section B-B', at 5.5 m depth inside the Y-Cave, are shown in Figure 10. The mass fraction of detrital terrigenous

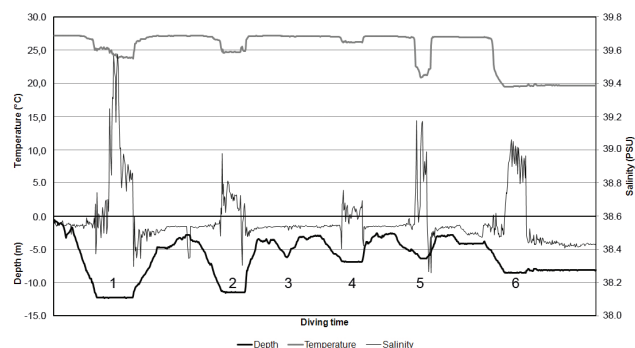


Fig. 8: Temperature, salinity and depth profiles recorded with the CTD probe during a dive inside the Y-Cave (August 27, 2003), 1 – vertical profile at the cave opening; 2 – vertical profile inside the cave entrance part; 3 – vertical profile at the turning point, section C-C'; 4 to 6 – vertical profiles in the inner part of the cave: 4 at approximately section E-E', 5 at approximately section G-G' and 6 at approximately section H-H'.

sediment (gravel >4 mm) was the highest (48.8%). The volume fractions of the four categories were very similar to the mass fractions. The shells of the gastropod *Homalopoma sanguineum* comprised a significant portion of the sediment (mass fraction 10.3%, volume fraction 13.0%).

Dissolutional effect

The potential presence of the aggressive SGD was primarily recognized through the corrosion marks on speleothems and bedrock (Fig. 11). In addition, there was a significant absence/scarcity of sessile marine organisms near the sea surface in the chamber with speleothems and air pocket and on the cave ceiling throughout the entire inner part of the cave (Fig. 11, B-D). The results of the subsequent 1-year dissolution experiment on the limestone tablets are shown in Table 1 and Figure 12. Since the methodology refers to the amount of carbonate dissolution, positive values suggest an enhanced mass loss while negative values indicate an increase in tablet mass. The most pronounced

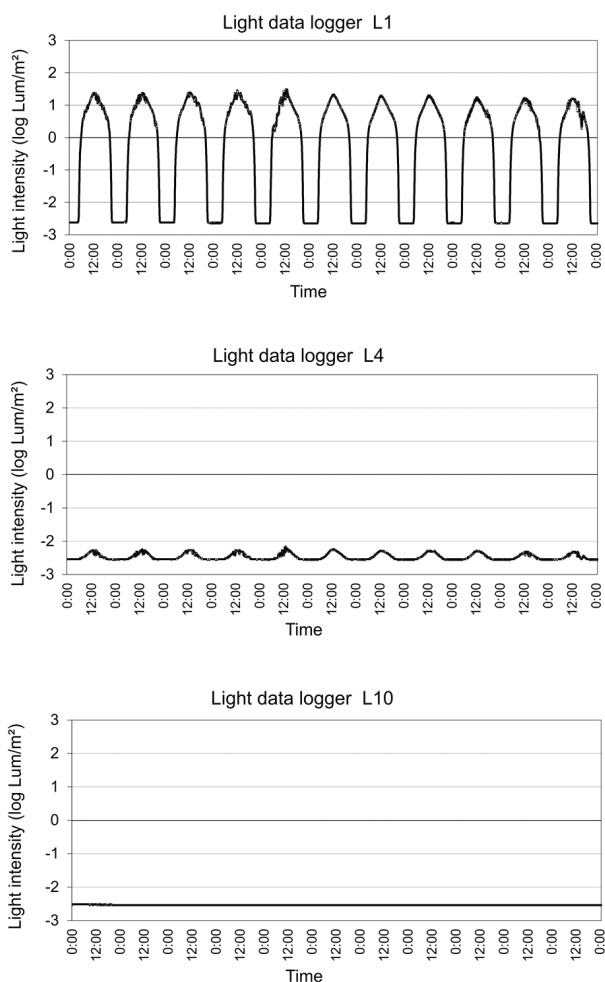


Fig. 9: Variation of light intensity over a period of 11 days (June 19–30, 2006) at representative sites within the Y-Cave (Fig. 3): logger 1 – the entrance of the cave; logger 4 – the central part of the cave; logger 10 – the innermost part of the cave.

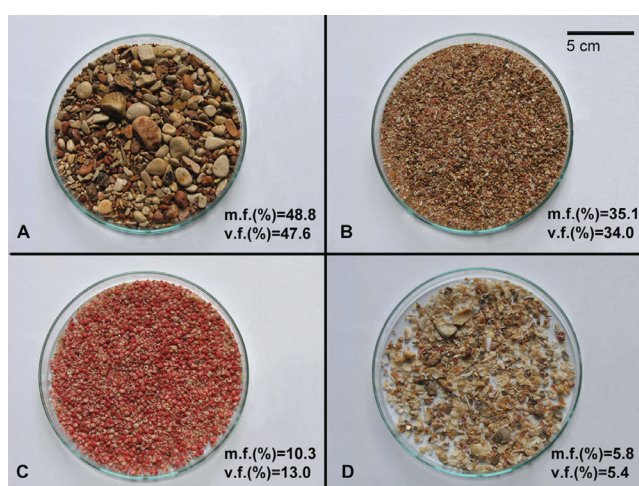


Fig. 10: The mass (m.f.) and volume fractions (v.f.) of four sediment categories in the sediment sample collected behind section B-B' (Fig. 2), at 5.5 m of depth inside the Y-Cave; A) detrital terrigenous sediment >4 mm, B) mixed biogenic and terrigenous detritus, C) shells of gastropod *Homalopoma sanguineum*, D) other biogenic material – shells, tests and skeletons of other marine organisms.

differences were the mass gain at site 1 at the entrance of the cave (Fig. 12, A) attributed to bioaccumulation, and the mass loss at site 6 at the end of the cave (Fig. 12, C) where all three tablets were visibly abraded. The absolute dissolution values are not comparable to any previous studies, as this was the first deployment of “standard” limestone tablets in a submarine environment.

Effect of hydrodynamics

The impact of the hydrodynamics within the cave is seen in the sediment particle size. The sediment on the bottom is coarser behind the section B-B' (Fig. 13) in the middle and at the very end of the cave (section H-H') than the sediment at the entrance (section A-A') and in the side channel in the middle of the cave (section C-C').

Discussion

In order to protect the cave biota in the Y-Cave, the relative abundance of the species was estimated rather than determined quantitatively and sampling was performed only as necessary. Although justified from the conservation point of view, this methodology has its limitations as it cannot assure that the sampling effort was uniform for all cave areas or all groups of organisms. However, even with the limited precision obtained with this methodology, a comparison of the collected data could be made and conclusions could be drawn.

The poriferan species diversity in the Y-Cave (56 taxa identified out of 139 in total; Appendix, Table 2) ranks among the ten highest when compared with other studied Mediterranean caves (Gerovasileiou & Voultsiadou, 2012, see Table S4). Mediterranean marine caves have been recognized as an important sponge biodiversity reservoir, with 45.7% of all recorded marine poriferan species also found in caves (311 of 681 species; Gerovasileiou & Voultsiadou, 2012). In a previous study, a total of 77 sponge species were found in 7 marine caves along the eastern Adriatic coast (Bakran-Petricioli *et al.*, 2012).

The distribution of sponges throughout the Y-Cave is positively correlated with the light gradient: the highest species diversity (45 of 56 taxa) was recorded in the front part of the cave where there is some light penetration (Fig. 9). That part of the cave, with over 100% biological cover (Fig. 4 A-D) and 122 taxa recorded, can be characterized as a typical GSO. In the middle and end parts of the cave (Fig. 4 E-H), which have virtually no light (Fig. 9), sponge diversity is much lower (21 taxa in the middle and 18 taxa in the end part) as is the relative abundance of sponge species. A decreasing number and abundance of sponge species along the horizontal cave axis has also been noted in many other superficial Mediterranean marine caves with blind ends (with a single entrance) (Cinelli *et al.*, 1977; Balduzzi *et al.*, 1989; Corriero *et al.*, 2000; Arko-Pijevac *et al.*, 2001; Gerovasileiou & Voultsiadou, 2012). It is widely

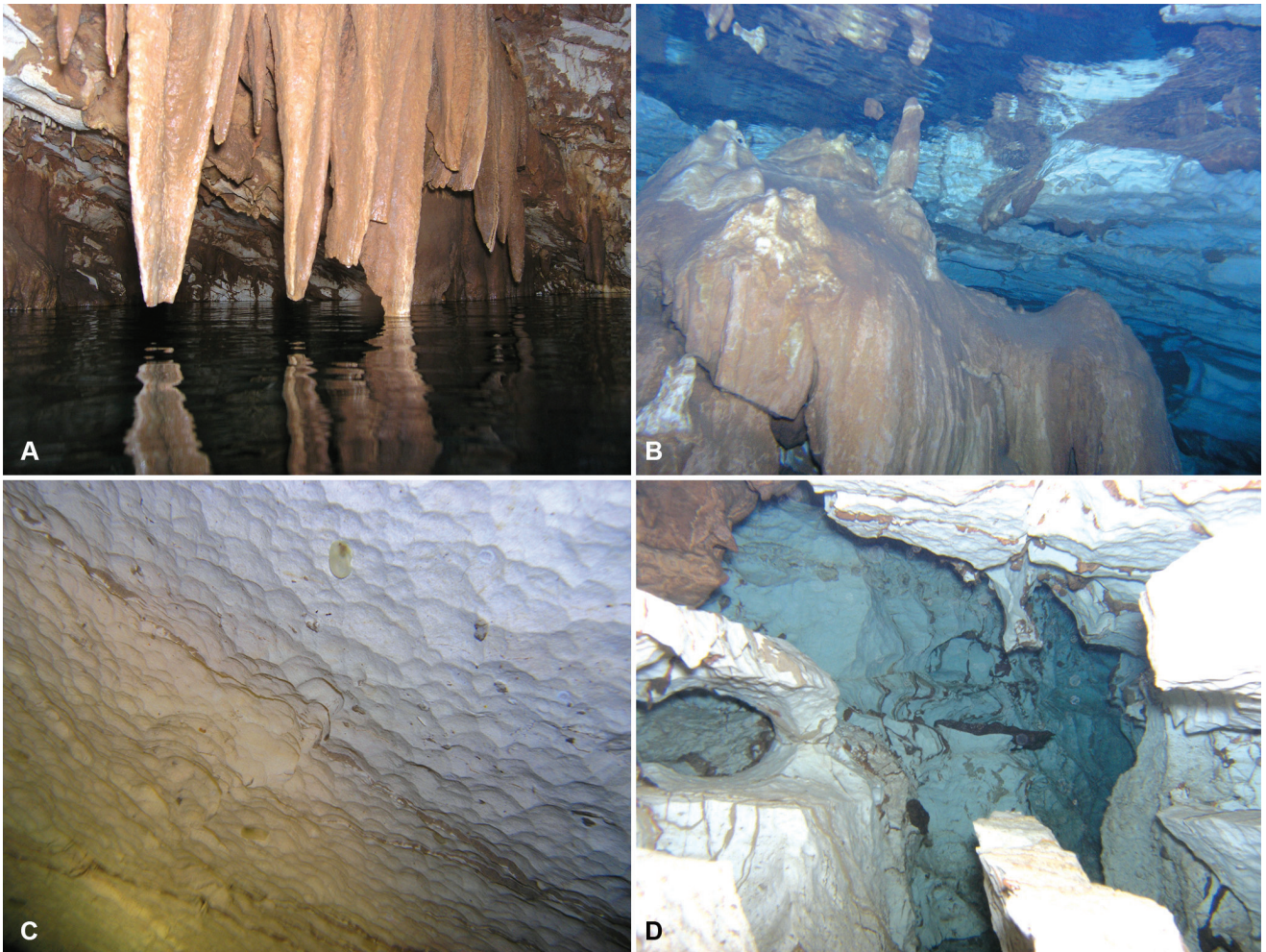


Fig. 11: Cave features: A) stalactites in the chamber with the air pocket (section C-C'); B) submerged stalagmites and flowstones with a lack of marine cave biota (section C-C'); C) submerged scallops (asymmetrical, cusped, oyster-shell-shaped dissolution depressions in the cave walls used as an indicator of flow direction; Murphy, 2012), (section D-D'); D) corroded cave walls (section F-F').

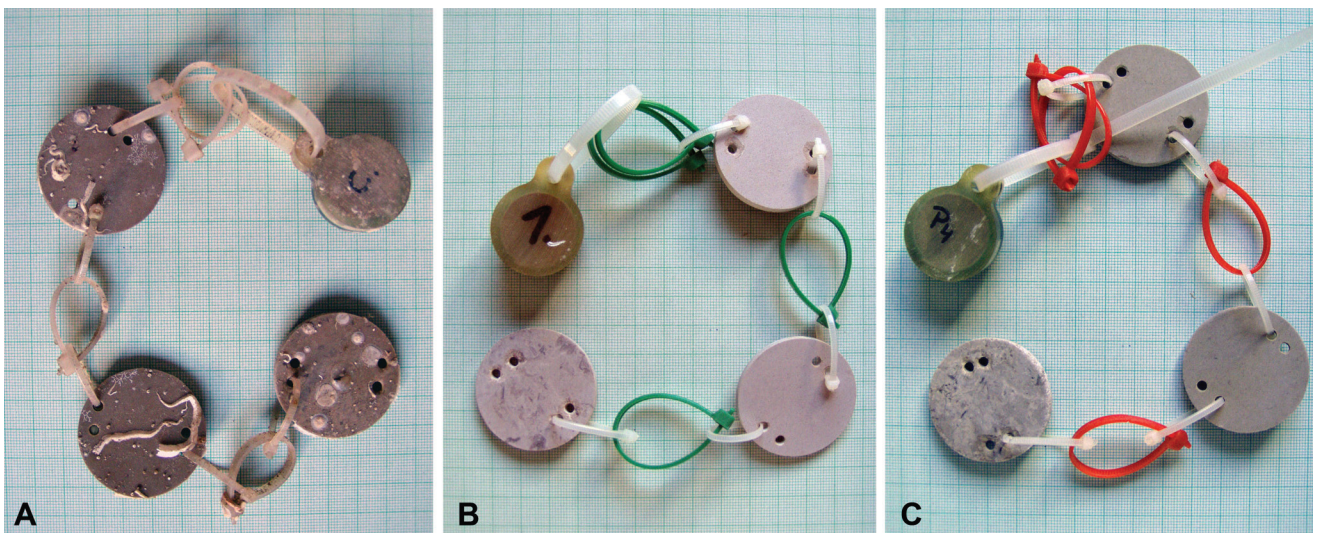


Fig. 12: Limestone tablets from the three representative sites after the 1-year exposure period: A) with bioaccumulation at site 1; B) corroded at site 3; C) abraded at site 6 (Fig. 3, Tab. 1).

accepted that such a distribution is strongly correlated not only with light attenuation but also with reduced water circulation. Harmelin (1969) stated that in dark tunnels (ducts open on both sides) with constant water renewal, a typical

GSO spreads into total darkness.

The middle and the end parts of the cave, which are characterized by an absence of light (Fig. 9), were the most similar in terms of their species diversity (taking all spe-



Fig. 13: The effect of hydrodynamics inside the Y-Cave, the location behind section B-B' (Fig. 2) at 5.5 m of depth, where the unusually coloured sediment sample was collected for analysis.

cies into account Q/S = 50.0%; taking only sponge species into account Q/S = 76.9%). Both parts could generally be assigned as GO due to their species composition, lower species diversity and abundance (Fig. 4 E-H). However, due to their biological peculiarities (discussed below), we decided to separate them into two zones: the middle part of the cave between sections C-C' and E-E' (Fig. 2), which we considered to be a transition zone from GSO to GO, and the end part of the cave from approximately section E-E' to the end of the cave, which we considered to be GO.

In the middle part of the cave, the diversity and relative abundance of species was higher than in the end part of the cave (42 vs. 20 taxa). A typical nodular type of bryozoan facies, considered as a transition from GSO to GO (Harmelin *et al.*, 1985), was noted only in small patches on vertical walls, between the sections C-C' and D-D'. The community on most vertical surfaces and overhangs in that area of the cave was dominated by serpulids (Fig. 4 F).

In the middle part of the cave, an abundant population of the small pink gastropod *Homalopoma sanguineum* (family Colloniidae) was noted (Appendix, Table 2) on the rocky walls and on individuals of the sponge *Spongia* (*Spongia*) *virgultosa*. The analysis of the coarse sediment collected behind the B-B' cross-section (at the beginning of the middle part of the cave; Fig. 2), at 5.5 m depth, showed that it contained a significant proportion of *Homalopoma* shells (Fig. 10 C). Arko-Pijevac *et al.* (2001) found that *H. sanguineum* dominated rock fissures below 2 m depth in a narrow vertical channel ("chimney") open to air in a marine cave in the northern Adriatic. Dantart & Luque (1994) stated that this species is common in marine caves (often more abundant in the interior) and also in coralligenous habitats of the Mediterranean. Although usually considered an algal herbivore, these results suggest that *H. sanguineum* can maintain abundant populations inside marine caves tens of meters from algal beds, likely feeding on sponges and organic detritus. This finding is in agreement with the results of an analysis of the gastropod digestive tract content by Dantart & Luque (1994), which contained

diatom tests, sponge spicules, fragments of hydroids and some unidentifiable detritus.

The discovery of a gregarious settlement of brachiopod *Novocrania anomala* on the walls in the middle part of the cave, between sections C-C' and D-D' (Fig. 4 G) is another interesting result. According to Jackson (2000), this species is gonochoristic and has lecithotrophic larvae. The fertilization is external and the eggs settle on the bottom. Free swimming larvae are fully developed within three days and settle on the substrate, cementing their ventral valves onto it within days. The species is an active filter feeder and is thought to prefer water currents at rates of less than one knot. This could explain the gregarious settlement of *N. anomala* in the Y-Cave. Gregarious settlements of only one or two species in cryptic habitats (lava caves) have been noted for some other species of brachiopods (Logan *et al.*, 2007). The brachiopod *N. anomala*, albeit not very common, is distributed along the eastern coast of the Adriatic Sea (Logan, 2003; Legac, 2012). However, such a gregarious settlement like the one found in this cave has not previously been reported for this species. Although Logan (2003) and Legac (2012) consider the specimens found in the northern Adriatic to be a separate species (*Novocrania turbinata*), a recent study by Emig (2014) showed that *N. turbinata* is actually a synonym of *N. anomala*, the latter being the valid name for this species (Costello *et al.*, 2014).

In their research on fish assemblages in three shallow marine caves with a single entrance (similar morphology to the Y-Cave), Bussotti *et al.* (2002) recorded a total of 19 fish species (per cave: 12, 12 and 10 species). They noted a decrease of fish species richness and abundance along the horizontal axes of the caves (except for *A. imberbis*). Due to the methodology used in our research, fish assemblages within the Y-Cave can not be discussed in detail, the species recorded (10 common species), their number and relative abundance along the cave are in concordance with the results of Bussotti *et al.* (2002).

Virtually no sessile marine organisms were noted on the walls within the Y-Cave shallower than 2 m depth (Fig. 11). This absence could be attributed to the freshwater influence in the upper layers of the water column inside the cave. Comparable observations have been made in submarine caves from SE Sicily (Guido *et al.*, 2013; Sanfilippo *et al.*, 2014). Although freshwater discharge was noted from the fissure at the entrance of the cave at 6 m depth (February 2006) there are no notable signs of freshwater impact on the anthozoan populations of GSO that inhabit the ceiling and overhangs in the entrance part (Fig. 4 B-C, depths 6 and 7 m respectively). Further in the cave, at shallower depths, the absence/scarcity of benthic organisms and pronounced corrosion marks suggest a freshwater influence. The existence and retention of colder surface water layers inside the chamber with speleothems and air pocket during most of summer 2004 (Fig. 5, logger 3) could only be explained by the less sa-

line character of that layer. Divers also noted a brackish layer approximately 10 cm thick on the sea surface inside the chamber in June 2006. Freshwater impact (flow, retention, mixing with sea water) in the upper layers of the water column inside shallow karstic caves could be a very important ecological factor that shapes the living communities within the caves, but which is often disregarded (Harmelin, 1986; Moscatello & Belmonte, 2007).

The dissolutional effect of SGD measured through differences in tablet masses after one year of exposure within the cave (Fig. 12, Table 1) led to the identification of three different, independent processes: i) bioaccumulation; ii) dissolution and iii) mechanical erosion. These processes are controlled by the position in the cave in relation to the distance from the entrance and the absolute depth that consequently generates different environmental conditions. An outline of each is provided below:

i) Bioaccumulation, owing to marine organisms that build carbonate skeletons, was pronounced in the entrance part of the cave and likely though to a smaller extent, along the inner, but not shallow part of the cave. After the 1-year exposure period, the limestone tablets were populated by serpulids, encrusting bryozoans and fouling bivalves. The abundance of bioconstructing organisms such as stony corals, branched and encrusting bryozoans, and serpulids, is much higher in the front part of the cave. Bioconstruction is common in the karst environment and plays an important role in shaping limestone coasts (De Waele & Furlani, 2013), cave interiors (Surić, 2005), and is an essential component of biokarst. Biokarst refers to depositional and erosional features produced by direct biological action (Viles, 1988; Bonacci *et al.*, 2009) and it is not unusual to have overlapping depositional and erosional components. Bioerosional processes also take part in the Y-Cave, as the endolithic bivalves *Lithophaga lithophaga* and *Rocellaria dubia*, and boring sponges from the genus *Cliona* were observed in the front and the middle parts of the cave.

ii) The dissolutional effect, i.e. mixing corrosion, was noticed in the shallowest part of the cave. According to the recorded geochemical activity of freshwater and the position of the cave, the development of the Y-Cave would fit into the Carbonate Island Karst Model (CIKM), which integrates various components that control cave and karst development on carbonate islands (Mylroie & Mylroie, 2007). The most pronounced features within the CIKM are the *flank margin caves* that develop by mixing dissolution at the boundary between saltwater and the overlying freshwater lens, and also at the contact of the vadose and phreatic zones at the top of the freshwater lens. The two zones where mixing occurs are superimposed at the distal margin of the freshwater lens, where the lens thins and creates an additive geochemical effect (Mylroie & Mylroie, 2007; Otoničar *et al.*, 2010). The Y-Cave is located within this zone. However, one of the principles of the CIKM is that the karst is eogenetic (i.e. diagenetically immature, young carbonate rocks that

have never been buried below the zone of meteoric diagenesis) or highly tectonized telogenetic karst (diagenetically mature, sometimes recrystallized rock with a lack of significant primary porosity) (Mylroie & Mylroie, 2007; Mylroie *et al.*, 2008). The Croatian coastal karst is generally telogenetic and flank margin caves are not expected to be found. The Plava Grota Cave (Cres Island) is an exception: it was formed in talus breccias facies, which provides three-dimensional porosity and permeability structure that acts hydraulically similar to the high primary porosity and permeability of young eogenetic carbonate rocks (Otoničar *et al.*, 2010). Still, the bedrock of the Y-Cave is neither highly-tectonized nor breccia, so dissolution is not pronounced enough to form a maze-like cave or larger chambers. However, it is strong enough to affect the bedrock surface, and thus might be an important factor in the biological species distribution.

iii) Mechanical erosion due to the impact of hydrodynamism is pronounced at the very end of the cave, almost 90 meters from the entrance. The relatively wide submerged cave entrance (7 m) at 12 m depth faces the open sea (Fig. 2). The aforementioned high wave energy produces a hydraulic impact inside the cave but, due to the cave morphology, the impact is not of the same intensity in all parts of the cave. This is registered in the different sediment particles size (coarser sediment inside the cave and at the end of it than at the entrance or in the side channel). The impact of abrasive forces was additionally seen in the abraded limestone tablets at the end of the cave (Fig. 12 C, Table 1) and even more so by the rounded gravel and polished surrounding bedrock 22 m from the entrance, as shown in Figures 10 and 13. A similar abrasion effect observed on shells was mentioned by Driscoll (1976). These visible consequences of a pronounced hydraulic impact coincide with the narrowing of the cave channels at these sites. This phenomenon is known as the “water ram” but it has not previously been described within karstic caves. Interestingly, the abraded carbonate tablets (coupled with temperature logger 6) were within the bottom cold water layer which persists in the cave during most of the year (Fig. 5, logger 6), meaning that the wave energy is transferred in such a way that it does not mix the water column, thus maintaining the water layers. That can also explain the scarcity of organisms in the marine layer at the end of the cave despite the pronounced hydrodynamism – although wave energy is transferred, there is actually no food transport that reaches the end of the cave.

The stratification of the water column within the cave throughout most of the year is shown in Figure 5. First, the retention of a colder water layer, especially throughout the summer, happens along the bottom inside the cave (Fig. 5, logger 6). There was a pronounced thermocline, with a sudden temperature drop of 7°C in the summer at approximately 5 m depth (Fig. 7), which could clearly be attributed to the cave morphology (Fig. 2). The vertical profiles showed that the salinity of the cold water layer

was similar to that of the open sea (Fig. 8, profiles 4, 5 and 6). This phenomenon could have a significant impact on marine biota as deep sea sponges have been found elsewhere in cold water lenses on the bottom of shallow caves (Bakran-Petricioli *et al.*, 2007). Second, the retention of cold, apparently brackish waters on the sea surface in the speleothem chamber during summer (Fig. 5, logger 3) is in accordance with the absence of marine organisms shallower than 2 m depth inside the cave (Fig. 11) and suggests a freshwater impact. Third, the retention of warmer water in the upper parts of the cave in the winter was noted (Fig. 5, loggers 2, 3 and 5), which could also suggest the possible mixing of freshwater and seawater.

The freshwater outflow from the Y-Cave certainly results in compensating seawater inflow though its extent cannot be estimated. This phenomenon was reported earlier in the stratified karstic estuary of the Krka River (Legović *et al.*, 1991), and in the freshwater outlet of a hydropower plant in Croatia (Legović *et al.*, 2003). The compensating inflow of seawater could bring more food to the marine organisms within the cave.

The year round measurement of water temperature revealed a peculiar phenomenon in the middle of the cave: rapid periodical changes of water temperature at 5 m depth during the winter (Fig. 5, logger 4). These oscillations are undoubtedly connected to the tides, as the temperature rises with each low tide and the temperature drops with each high tide, by approximately 3°C (Fig. 6). It can be presumed that with each high tide, a wedge of outside seawater, which is less dense than the cold water in the cave but denser than the upper layer (and likely less saline), penetrates into the cave, at least to its middle part. This daily tidal dynamic could bring more food to marine organisms in the middle part of the cave (evidenced by the dense population of the gastropod *Homalopoma sanguineum* and the gregarious settlement of the brachiopod *Novocrania anomala*), though it is not strong enough to disturb the inner stratification of the cave.

The temperature oscillations recorded during the summer months at the entrance of the cave at 11.5 m depth (Fig. 5, logger 1) are due to a phenomenon that was first recorded in the southern Adriatic. Novosel *et al.* (2004) found that marine life within the thermocline layer is exposed to large high-frequency oscillations connected partly to an internal diurnal tide. Similar oscillations could be noticed inside the cave at loggers 2, 4 and 5 (depths 2.9 m, 5.1 m and 3.9 m respectively) but not at loggers 3 (depth 0.7 m) and 6 (depth 8.5 m). Those summer oscillations did not disturb the stratification of the water column inside the cave.

Conclusions

The distribution of living organisms along the Y-Cave, together with the results of the measured abiotic parameters, clearly reflects the complex environmental conditions that shape this shallow, partly submerged

coastal cave at a small (meter) scale. The phylum Porifera was the dominant group of organisms and the poriferan species diversity in the Y-Cave ranked among the ten highest of all other investigated Mediterranean caves. The general distribution of organisms along the Y-Cave is positively correlated to the light gradient and reduced water circulation, thus the highest species diversity and abundance were recorded in the front part of the cave. The strong hydrodynamism evidenced at the end of cave is produced by wave energy transfer inside the cave and does not necessarily mean that there is transport of food (water circulation) all the way to the end of the cave.

Although the middle and end parts of the cave, both characterized by an absence of light, were the most similar, the biological peculiarities of the former, such as an abundant population of the gastropod *Homalopoma sanguineum* and a gregarious settlement of the brachiopod *Novocrania anomala*, are interpreted to be caused by differences in environmental factors, e.g. tidally generated hydrodynamics.

The absence/scarcity of sessile marine organisms and pronounced corrosion marks at shallow depths inside the Y-Cave suggest a freshwater impact (flow, retention, mixing with sea water) in the upper layers of the water column. That impact, often disregarded, plays an important role in the distribution of organisms in the cave, either due to unfavourable salinity or a corrosive impact.

The one-year experiment with carbonate tablets, aimed at detecting the dissolutional effect of seawater and freshwater mixing, revealed three different, independent ongoing processes controlled by the position in the cave in terms of distance from the entrance, absolute depth and cave morphology: i) bioaccumulation due to the construction of carbonate skeletons that was most pronounced in the entrance part; ii) dissolution due to mixing corrosion observed in the shallowest part of the cave; and iii) mechanical erosion due to the impact of hydrodynamism pronounced in different parts of the cave and associated with the cave morphology.

The results also revealed water column stratification within the cave: i) retention of a colder water layer, especially throughout the summer, along the bottom of the cave interior, which is associated with the cave morphology, ii) retention of cold, apparently brackish water, on the sea surface in the speleothem chamber during summer, iii) retention of warmer water in upper parts of the cave in winter which could be attributed to the possible mixing of freshwater and seawater. Although the cave is shallow and exposed to the open sea, neither tidal nor wave energy, both observed at particular sites within the cave, disturb the stratification.

In addition to the hydrologically induced geochemical changes, even small differences in the morphology of a simple, shallow marine cave could have ecological implications that could easily be overlooked without simultaneous long-term measurements of key abiotic parameters, such as temperature, salinity, light, and hydro-

dynamism in distinct spots inside the cave. The present study shows that the resulting distribution of organisms within the Y-Cave is unique to the cave and confirms the necessity of considering this fact where the conservation and management of marine caves are concerned.

Acknowledgements

We are grateful to M. Juračić for fruitful discussion on karstification in marine caves; to M. Juračić, S. Dujmović and H. Čizmek for help in underwater observation and sampling; to V. Tomišić for laboratory work on carbonate tablets. We also thank Oikon Ltd Institute for Applied Ecology for the use of the Idronaut Ocean Seven 316 CTD probe for diving profiles in the Y-Cave on August 27, 2003. The data from the Zadar tide gauge was kindly provided by the Croatian Hydrographic Institute (2012). This research was partially funded by the Ministry of Science, Education and Sport of the Republic of Croatia (Projects no. 119-0362975-1226 and 269-2693084-3083). We would also like to thank three independent reviewers for their valuable comments and suggestions.

References

- Arko-Pijevac, M., Benac, Č., Kovačić, M., Kirinčić, M., 2001. A submarine cave at the Island of Krk (North Adriatic Sea). *Natura Croatica*, 10 (3), 163-184.
- Bakran-Petricioli, T., 2011. 8330 Submerged or partially submerged marine caves. p. 160-173. In: *Manual for determination of marine habitats in Croatia according to Habitat Directive*. State Institute for Nature Protection, Zagreb.
- Bakran-Petricioli, T., Petricioli, D., 2008. Habitats in submerged karst of Eastern Adriatic coast - Croatian natural heritage. *Croatian Medical Journal*, 49 (4), 455-458.
- Bakran-Petricioli, T., Radolović, M., Petricioli, D., 2012. How diverse is sponge fauna in the Adriatic Sea? *Zootaxa*, 3172, 20-38.
- Bakran-Petricioli, T., Vacelet, J., Zibrowius, H., Petricioli, D., Chevaldonné, P. *et al.*, 2007. New data on the distribution of the «deep-sea» sponges *Asbestopluma hypogea* and *Oopsacas minuta* in the Mediterranean Sea. *Marine Ecology*, 28 (Suppl. 1), 10-23.
- Balduzzi, A., Bianchi, C.N., Boero, F., Cattaneo-Vietti, R., Pansini, M. *et al.*, 1989. The suspension-feeder communities of a Mediterranean sea cave. *Topics in marine biology, Scientia Marina*, 53 (2-3), 387-395.
- Benedetti-Cecchi, L., Airoldi, L., Abbiati, M., Cinelli, F., 1996. Exploring the causes of spatial variation in an assemblage of benthic invertebrates from a submarine cave with sulphur springs. *Journal of Experimental Marine Biology and Ecology*, 208, 153-168.
- Bianchi, C.N., Morri, C., 1994. Studio bionomico comparativo di alcune grotte marine sommerse: definizione di una scala di confinamento. *Memoria di Istituto Italiano di Speleologia*, 6 (II), 107-123.
- Bianchi, C.N., Cattaneo-Vietti, R., Cinelli, F., Morri, C., Pansini, M., 1996. Lo studio biologico delle grotte sottomarine del Mediterraneo: conoscenze attuali e prospettive. *Bollettino dei Musei e degli Istituti Biologici dell'Università di Genova*, 60-61, 41-69.
- Bögli, A., 1964. Mischungskorrosion: ein Beitrag zum Verkarstungsproblem. *Erdkunde*, 18, 83-92.
- Bokuniewicz, H., Buddemeier, R., Maxwell, B., Smith, C., 2003. The typological approach to submarine groundwater discharge (SGD). *Biogeochemistry*, 66 (1/2), 145-158.
- Bonacci, O., Pipan, T., Culver, D.C., 2009. A framework for karst ecohydrology. *Environmental Geology*, 56 (5), 891-900.
- Burnett, W.C., Bokuniewicz, H., Huettel, M., Moore, W.S., Taniguchi, M., 2003. Groundwater and pore water inputs to the coastal zone. *Biogeochemistry*, 66 (1-2), 3-33.
- Bussotti, S., Denitto, F., Guidetti, P., Belmonte, G., 2002. Fish assemblages in shallow marine caves in the Salento Peninsula (southern Apulia, SE Italy). *Marine Ecology*, 23 (suppl. 1), 11-20.
- Bussotti, S., Terlizzi, A., Fraschetti, S., Belmonte, G., Boero, F., 2006. Spatial and temporal variability of sessile benthos in shallow Mediterranean marine caves. *Marine Ecology Progress Series*, 325, 109-119.
- Buzjak, N., Petković, A., Faivre, S., 2013. The intensity of increment and of subcutaneous karst corrosion in the Krka River valley (Croatia) (in Croatian). *Hrvatski geografski glasnik*, 75 (2), 59-79.
- Chevaldonné, P., Lejeune, C., 2003. Regional warming-induced species shift in north-west Mediterranean marine caves. *Ecology Letters*, 6, 371-379.
- Cinelli, F., Fresi, E., Mazzella, L., Pansini, M., Pronzato, R. *et al.*, 1977. Distribution of benthic phyto- and zoocoenoses along a light gradient in a superficial marine cave. p. 173-183. In: *Biology of benthic organisms, Proceedings of the Eleventh European Symposium on Marine Biology, University College, Galway, 5-11 October 1976*. Keegan, B.F., Ceidigh, P.O., Boaden, P.J.S. (Eds). Pergamon Press, Oxford.
- Corriero, G., Scalera Liaci, L., Ruggiero, D., Pansini, M., 2000. The sponge community of a semi-submerged Mediterranean cave. *Marine Ecology*, 21 (1), 85-96.
- Costello, M.J., Bouchet, P., Boxshall, G., Arvanitidis, C., Appeltans, W. 2014. *European Register of Marine Species (ERMS)*. <http://www.marbef.org/data/erms.php> (Accessed November 14, 2014)
- Cushman-Roisin, B., Gacic, M., Poulain, P.-M., Artegiani, A. 2001. *Physical Oceanography of the Adriatic Sea: Past, Present and Future*. Kluwer Academic Publishers, Dordrecht/Boston/London, 304 pp.
- Dantart, L., Luque, A.A., 1994. Notas sobre *Homalopoma sanguineum* (Linnaeus, 1758) (Gastropoda, Archaeogastropoda, Turbinidae). *Iberus (Revista de la Sociedad Española de Malacología)*, 12 (2), 77-82.
- De Waele, J., Furlani, S., 2013. Seawater and Biokarst Effects on Coastal Limestones. p. 341-350. In: *Treatise on Geomorphology 6*. Shroder, J.F. (Ed.). Academic Press, San Diego.
- Driscoll, E.G., 1976. Experimental Field Study of Shell Abrasion. *Journal of Sedimentary Research*, 37 (4), 1117-1123.
- Emig, C.C., 2014. *Novocrania turbinata* synonyme de *N. anomala*. *Carnets de Géologie (Notebooks on Geology)*, 14 (8), 159-171.
- Fairchild, I.J., Baker, A., 2012. *Speleothem Science: From Process to Past Environments*. Wiley-Blackwell, Chichester, 432 pp.
- Frank, E.F., Mylroie, J., Troester, J., Calvin Alexander Jr., E., Carew, J.L., 1998. Karst development and speleogenesis, Isla de Mona, Puerto Rico. *Journal of Cave and Karst*

- Studies*, 60 (2), 73-83.
- Fuček, L., Jelaska, V., Gušić, I., Prtoljan, B., Oštrić, N., 1991. Padinski sedimenti uvale Brbišnica na Dugom otoku (Turonian slope deposits in the Brbišnica Cove, Dugi otok Island, Croatia). *Geološki vjesnik*, 44, 55-67.
- Gabrovšek, F., 2009. On concepts and methods for the estimation of dissolutional denudation rates in karst areas. *Geomorphology*, 106 (1-2), 9-14.
- Gabrovšek, F., Dreybrodt, W., 2010. Karstification in unconfined limestone aquifers by mixing of phreatic water with surface water from a local input: a model. *Journal of Hydrology*, 386 (1-4), 130-141.
- Gams, I., 1985. International comparative measurements of surface solution by means of standard limestone tablets. *Zbornik Ivana Rakovca*, XXVI, 361-386.
- Gerovasileiou, V., Voultziadou, E., 2012. Marine caves of the Mediterranean Sea: A sponge biodiversity reservoir within a biodiversity hotspot. *PLoS ONE* 7(7), e39873. doi:10.1371/journal.pone.0039873
- Giakoumi, S., Sini, M., Gerovasileiou, V., Mazor, T., Beher, J. et al., 2013. Ecoregion-based conservation planning in the Mediterranean: Dealing with large-scale heterogeneity. *PLoS ONE* 8 (10), e76449. doi:10.1371/journal.pone.0076449
- Gili, J.M., Riera, T., Zabala, M., 1986. Physical and biological gradients in a submarine cave on the Western Mediterranean coast (north-east Spain). *Marine Biology*, 90, 291-297.
- Gillieson, D.S., 1996. *Caves: processes, development and management*. Blackwell. Cambridge, xii + 324 pp.
- Guarnieri, G., Terlizzi, A., Bevilacqua, S., Fraschetti, S., 2012. Increasing heterogeneity of sensitive assemblages as a consequence of human impact in submarine caves. *Marine Biology*, 159, 1155-1164.
- Guido, A., Heindel, K., Birgel, D., Rosso, A., Mastandrea, A. et al., 2013. Pendant bioconstructions cemented by microbial carbonate in submerged marine caves (Holocene, SE Sicily). *Paleogeography, Palaeoclimatology, Palaeoecology*, 388, 166-180.
- Harmelin, J.G., 1969. Bryozoaires des grottes sous-marines obscures de la région marseillaise, faunistique et écologie. *Téthys*, 1 (3), 793-806.
- Harmelin, J.G., 1986. Patterns in the distribution of Bryozoans in the Mediterranean marine caves. *Stygologia*, 2 (1-2), 10-25.
- Harmelin, J.G., 1997. Diversity of bryozoans in a Mediterranean sublittoral cave with bathyal-like conditions: role of dispersal processes and local factors. *Marine Ecology Progress Series*, 153, 139-152.
- Harmelin, J.G., Vacelet, J., Vasseur, P., 1985. Les grottes sous-marines obscures: un milieu extreme et un remarquable biotope refuge. *Téthys*, 11 (3-4), 214-229.
- HHI (Croatian Hydrographic Institute), 2012. *Peljar I: Jadransko more - istočna obala (5th edn.)*, Hrvatski hidrografski institut, Split.
- Hooper, J.N.A., Van Soest, R.W.M. (Eds), 2002. *Systema Porifera, A Guide to the Classification of Sponges*. Kluwer Academic/Plenum Publishers, New York, 1763 pp.
- Jackson, A., 2000. *Neocrania anomala*. A brachiopod. *Marine Life Information Network: Biology and Sensitivity Key Information Sub-programme. Plymouth: Marine Biological Association of the United Kingdom*. <http://www.marlin.ac.uk/reproduction.php?speciesID=3879> (Accessed November 14, 2014)
- Janssen, A., Chevaldonné, P., Martínez Arbizu, P., 2013. Meiobenthic copepod fauna of a marine cave (NW Mediterranean) closely resembles that of deep-sea communities. *Marine Ecology Progress Series*, 479, 99-113.
- Juračić, M., Bakran-Petricioli, T., Petricioli, D., 2002. Cessation of karstification due to the sea-level rise? Case study of the Y-cave, Dugi Otok, Croatia. p. 319-326. In: *Evolution of Karst: From Prekarst to Cessation, Symposium Proceedings, Postojna, 17-21 September 2002*, Gabrovšek, F. (Ed.). Inštitut za raziskovanje krasa, ZRC SAZU, Postojna.
- Kaufmann, G., Dreybrodt, W., 2007. Calcite dissolution kinetics in the system CaCO₃-H₂O-CaCO₃ at high undersaturation. *Geochimica et Cosmochimica Acta*, 71 (6), 1398-1417.
- Kennett, J.P., 1982. *Marine Geology*. Prentice-Hall, New Jersey, 813 pp.
- Krklec, K., Marjanac, T., Perica, D., 2013. Analysis of "standard" (Lipica) limestone tablets and their weathering by carbonate staining and SEM imaging, a case study on the Vis Island, Croatia. *Acta Carsologica*, 42 (1), 135-142.
- Laborel, J., Vacelet, J., 1959. Les grottes sous-marines en Méditerranée. *Comptes Rendus de l'Académie des Sciences Paris*, 248, 2619-2621.
- Leder, N., Smirčić, A., Vilibić, I., 1998. Extreme values of surface wave heights in the Northern Adriatic. *Geofizika*, 15, 1-13.
- Legac, M., 2012. New records of recent Brachiopoda from the eastern part of the northern Adriatic Sea. *Natura Croatica*, 21 (1), 255-258.
- Legović, T., Gržetić, Z., Smirčić, A., 1991. Effects of wind on a stratified estuary. *Marine Chemistry*, 32 (2/4), 153-161.
- Legović, T., Janeković, I., Viličić, D., Petricioli, D., Smoljan, Z., 2003. Effects of freshwater release to a marine bay. *Journal of Environmental Science and Health Part A - Toxic/Hazardous Substances & Environmental Engineering*, A38 (8), 1411-1420.
- Logan, A., 2003. Marine fauna of the Mljet National Park (Adriatic Sea, Croatia). 3. Brachiopoda. *Natura Croatica*, 12 (4), 233-243.
- Logan, A., Wirtz, P., Swinnen, F., 2007. New record of *Novocrania* (Brachiopoda, Craniida) from Madeira, with notes on recent brachiopod occurrences in the Macaronesian archipelagos. *Arquipélago - Life and Marine Sciences*, 24, 17-22.
- Lovato, T., Androsov, A., Romanenkov, D., Rubino, A., 2010. The tidal and wind induced hydrodynamics of the composite system Adriatic Sea/Lagoon of Venice. *Continental Shelf Research*, 30 (6), 692-706.
- Martí, R., Uriz, M.J., Ballesteros, E., Turon, X., 2004. Benthic assemblages in two Mediterranean caves: Species diversity and coverage as a function of abiotic parameters and geographic distance. *Journal of the Marine Biological Association of the UK*, 84, 557-572.
- Moscattello, S., Belmonte, G., 2007. The plankton of a shallow submarine cave ('Grotta di Ciolo', Salento Peninsula, SE Italy). *Marine Ecology*, 28 (Suppl. 1), 47-59.
- Murphy, P.J., 2012. Scallops. p. 679-683. In: *Encyclopedia of Caves (2nd edn.)*. Culver, D.C., White, W.B. (Eds.). Academic Press, Amsterdam.
- Mylroie, J.R., Mylroie, J.E., 2007. Development of the carbonate island karst model. *Journal of Cave and Karst Studies*, 69 (1), 59-75.
- Mylroie, J.E., Mylroie, J.R., Nelson, C.N., 2008. Flank Margin Cave Development in Telogenetic Limestones of New

- Zealand. *Acta Carsologica*, 37 (1), 15-40.
- Novosel, M., Požar-Domac, A., Pasarić, M. 2004. Diversity and distribution of the Bryozoa along underwater cliffs in the Adriatic Sea with special reference to thermal regime. *Marine Ecology*, 25 (2), 155-170.
- Otoničar, B., Buzjak, N., Mylorie, J., Mylorie, J., 2010. Flank margin cave development in carbonate talus breccia facies: An example from Cres Island, Croatia. *Acta Carsologica*, 39 (1), 79-91.
- Parravicini, V., Guidetti, P., Morri, C., Montefalcone, M., Donato, M. *et al.*, 2010. Consequences of sea water temperature anomalies on a Mediterranean submarine cave ecosystem. *Estuarine, Coastal and Shelf Science*, 86, 276-282.
- Pères, J.-M., Picard, J., 1964. Nouveau manuel de bionomie benthique de la Mer Méditerranée. *Recueil des Travaux de la Station Marine d'Endoume*, 47 (Bulletin 31), 5-137.
- Pikelj, K., Juračić, M., 2013. Eastern Adriatic Coast (EAC): geomorphology and coastal vulnerability of a karstic coast. *Journal of Coastal Research*, 29 (4), 944-957.
- Plan, L., 2005. Factors controlling carbonate dissolution rates quantified in a field test in the Austrian Alps. *Geomorphology*, 68, 201-212.
- Rastorgueff, P.-A., Harmelin-Vivien, M., Richard, P., Chevalloné, P., 2011. Feeding strategies and resource partitioning mitigate the effects of oligotrophy for marine cave mysids. *Marine Ecology Progress Series*, 440, 163-176.
- Riedl, R., 1966. *Biologie der Meereshöhlen*. Paul Parey, Hamburg and Berlin, 636 pp.
- Rosso, A., Di Martino, E., Sanfilippo, R., Di Martino, V., 2012. Bryozoan communities and thanatocoenoses from submarine caves in the Plemmirio marine protected area (SE Sicily). In: *Bryozoan Studies 2010. Proceedings of the 15th IBA Conference, Kiel, Germany, 2010*, Ernst, A., Schäfer, P., & Scholz, J. (Eds). Lecture Notes in Earth System Sciences (Springer, Berlin, Heidelberg), 143, 251-269.
- Rosso, A., Sanfilippo, R., Taddei Ruggiero, E., Di Martino, E., 2013. Serpuloidean, bryozoan and brachiopod faunas from submarine caves in Sicily. *Bollettino Società Paleontologica Italiana*, 52 (3), 167-176.
- Sanfilippo, R., Rosso, A., Guido, A., Mastandrea, A., Russo, F. *et al.*, 2014. Metazoan/microbial biostalactites from present-day submarine caves in the Mediterranean Sea. *Marine Ecology*, doi: 10.1111/maec.12229.
- Surić, M., 2005. Submerged karst – dead or alive? Examples from the Eastern Adriatic Coast (Croatia). *Geoadria*, 10(1), 5-19.
- Surić, M., Juračić, M., Horvatinčić, N., Krajcar Bronić, I., 2005. Late Pleistocene - Holocene sea-level rise and the pattern of coastal karst inundation: records from submerged speleothems along the Eastern Adriatic Coast (Croatia). *Marine Geology*, 214 (1-3), 163-175.
- Surić, M., Lončarić, R., Lončar, N., 2010. Submerged caves of Croatia - distribution, classification and origin. *Environmental Earth Sciences*, 61 (7), 1473-1480.
- Terzić, J., Peh, Z., Marković, T., 2010. Hydrochemical properties of transition zone between fresh groundwater and seawater in karst environment of the Adriatic islands, Croatia. *Environmental Earth Sciences*, 59 (8), 1629-1642.
- Terzić, J., Šumanovac, F., Buljan, R., 2007. An assessment of hydrogeological parameters on the karstic island of Dugi Otok, Croatia. *Journal of Hydrology*, 343 (1-2), 29-42.
- Vacelet, J., Boury-Esnault, N., Harmelin, J.G., 1994. Hexactinellid Cave, a unique deep-sea habitat in the scuba zone. *Deep-Sea Research Part I*, 41 (7), 965-973.
- Van Hengstum, P.J., Scott, D.B., Gröcke, D.R., Charette, M.A., 2011. Sea level controls sedimentation and environments in coastal caves and sinkholes. *Marine Geology*, 286, 35-50.
- Van Soest, R.W.M., Boury-Esnault, N., Hooper, J.N.A., Rützler, K., de Voogd, N.J. *et al.*, 2014. *World Porifera database*. <http://www.marinespecies.org/porifera> (Accessed November 14, 2014)
- Viles, H.A., 1988. *Biogeomorphology*. Blackwell, Oxford, 365 pp.
- Vlahović, I., Tišljarić, J., Velić, I., Matičec, D., 2005. Evolution of the Adriatic Carbonate Platform: Palaeogeography, main events and depositional dynamics. *Palaeogeography, Palaeoclimatology, Palaeoecology*, 200, 333-360.
- Zabala, M., Riera, T., Gili, J.M., Barangé, M., Lobo, A. *et al.*, 1989. Water flow, trophic depletion, and benthic macrofauna impoverishment in a submarine cave from the Western Mediterranean. *Marine Ecology*, 10 (3), 271-287.
- Zhang, C., 2011. Carbonate rock dissolution rates in different landuses and their carbon sink effect. *Chinese Science Bulletin*, 56, 3759-3765.

APPENDIX

Table 2. List of the taxa collected and/or identified from photos in the Y-Cave, Dugi Otok Island, Croatia with their relative abundance (front part encompasses part of the cave from the entrance to approximately section C-C', middle part encompasses part from the section C-C' to the section E-E' and the end part encompasses part from the section E-E' to the end of the cave, see Figure 2 for the position of sections; relative abundance: cc - abundant species, c - common species, + - rare species).

Taxa	front part of the cave	middle part of the cave	end part of the cave
Chlorophyta			
<i>Palmophyllum crassum</i> (Naccari) Rabenhorst, 1868	c		
<i>Valonia utricularis</i> (Roth) C. Agardh, 1823	+		
Rhodophyta			
<i>Lithophyllum stictaeforme</i> (Areschoug) Hauck, 1877	+		
<i>Peyssonnelia rubra</i> (Greville) J. Agardh, 1851	c		
<i>Peyssonnelia squamaria</i> (S.G.Gmelin) Decaisne, 1842	c		
Foraminifera			
<i>Miniacina miniacea</i> (Pallas, 1766)	c	c	
Porifera			
<i>Amphoriscus chrysalis</i> (Schmidt, 1864)			c
<i>Clathrina clathrus</i> (Schmidt, 1864)	c	c	
<i>Clathrina coriacea</i> (Montagu, 1814)	c		
<i>Sycon elegans</i> (Bowerbank, 1845)		c	c
<i>Sycon raphanus</i> Schmidt, 1862		+	+
<i>Sycon</i> sp.		+	c
<i>Acanthella acuta</i> Schmidt, 1862	c		
<i>Agelas oroides</i> (Schmidt, 1864)	cc		
<i>Axinella cannabina</i> (Esper, 1794)	+		
<i>Axinella damicornis</i> (Esper, 1794)	+		
<i>Axinella verrucosa</i> (Esper, 1794)	c		
<i>Caminella intuta</i> (Topsent, 1892)		+	
<i>Chondrosia reniformis</i> Nardo, 1847	c	c	+
<i>Cliona celata</i> Grant, 1826	+		
<i>Cliona rhodensis</i> Rützler & Bromley, 1981		+	
<i>Cliona schmidti</i> (Ridley, 1881)	cc	c	
<i>Crambe crambe</i> (Schmidt, 1862)	c		
<i>Dictyonella incisa</i> (Schmidt, 1880)	c		
<i>Diplastrella bistellata</i> (Schmidt, 1862)	c	c	c
<i>Discodermia polymorpha</i> Pisera & Vacelet, 2011		+	+
<i>Dysidea avara</i> (Schmidt, 1862)	+		
<i>Dysidea fragilis</i> (Montagu, 1814)	c		
<i>Eurypon clavatum</i> (Bowerbank, 1866)	+		
<i>Geodia conchilega</i> Schmidt, 1862			+
<i>Haliclona (Halichoelona) fulva</i> (Topsent, 1893)	cc		
<i>Haliclona (Soestella) mucosa</i> (Griessinger, 1971)	cc		
<i>Hemimycale columella</i> (Bowerbank, 1874)	cc	+	
<i>Hymedesmia (Stylopus) coriacea</i> (Fristedt, 1885)	+		
<i>Ircinia dendroides</i> (Schmidt, 1862)	cc		
<i>Ircinia oros</i> (Schmidt, 1864)	c		
<i>Ircinia variabilis</i> (Schmidt, 1862)	cc		
<i>Jaspis johnstoni</i> (Schmidt, 1862)	+	+	+
<i>Merlia normani</i> Kirkpatrick, 1908	+		
<i>Myrmekioderma spelaeum</i> (Pulitzer-Finali, 1983)		c	c
<i>Penares euastrum</i> (Schmidt, 1868)	c		
<i>Petrosia (Petrosia) ficiformis</i> (Poiret, 1789)	cc	c	+
<i>Phorbas tenacior</i> (Topsent, 1925)	cc		
<i>Placospongia decorticans</i> (Hanitsch, 1895)		c	+
<i>Pleraplysilla spinifera</i> (Schulze, 1879)	+		
<i>Raspaciona aculeata</i> (Johnston, 1842)	+		
<i>Reniera</i> spp.	+		

(continued)

Table 2 (continued)

Taxa	front part of the cave	middle part of the cave	end part of the cave
<i>Rhabderemia spinosa</i> Topsent, 1896	+	+	+
<i>Sarcotragus foetidus</i> Schmidt, 1862	c		
<i>Sarcotragus spinosulus</i> Schmidt, 1862	c		
<i>Scalarispongia scalaris</i> (Schmidt, 1862)	cc		
<i>Spirastrella cunctatrix</i> Schmidt, 1868	cc	c	+
<i>Spongia (Spongia) officinalis</i> Linnaeus, 1759	+		
<i>Spongia (Spongia) virgultosa</i> (Schmidt, 1868)	+	c	+
<i>Spongosorites flavens</i> Pulitzer-Finali, 1983	+		
<i>Terpios gelatinosa</i> (Bowerbank, 1866)	+		
<i>Tethya aurantium</i> (Pallas, 1766)	+	+	
<i>Tethya</i> sp.			+
<i>Timea</i> sp.	+		
<i>Corticium candelabrum</i> Schmidt, 1862	c	c	+
<i>Oscarella lobularis</i> (Schmidt, 1862)	c		
<i>Plakina bowerbanki</i> (Sarà, 1960)	+	c	+
Cnidaria - Anthozoa			
<i>Balanophyllia (Balanophyllia) europaea</i> (Risso, 1826)	+		
<i>Caryophyllia (Caryophyllia) inornata</i> (Duncan, 1878)	+		
<i>Caryophyllia (Caryophyllia) smithii</i> Stokes & Broderip, 1828	+		
<i>Cerianthus membranaceus</i> (Spallanzani, 1784)	+		
<i>Isarachnanthus nocturnus</i> (Hartog, 1977)	+		
<i>Leptopsammia pruvoti</i> Lacaze-Duthiers, 1897	cc	c	
<i>Madracis pharensis</i> (Heller, 1868)	cc		
<i>Parazoanthus axinellae</i> (Schmidt, 1862)	c		
<i>Polycyathus muelleriae</i> (Abel, 1959)	c		
Echiura			
<i>Bonellia viridis</i> Rolando, 1821	+	+	
Mollusca - Gastropoda			
<i>Armina tigrina</i> Rafinesque, 1814	+		
<i>Berthella aurantiaca</i> (Risso, 1818)	+		
<i>Bolma rugosa</i> (Linnaeus, 1767)	+		
<i>Calliostoma zizyphinum</i> (Linnaeus, 1758)		+	
<i>Chromodoris</i> sp.	+		
<i>Clanculus corallinus</i> (Gmelin, 1791)	+		
<i>Conus ventricosus</i> Gmelin, 1791	+		
<i>Emarginula rosea</i> Bell, 1824	+		
<i>Flabellina affinis</i> (Gmelin, 1791)	+		
<i>Haliotis tuberculata</i> Linnaeus, 1758	+		
<i>Hexaplex trunculus</i> (Linnaeus, 1758)	+		
<i>Homalopoma sanguineum</i> (Linnaeus, 1758)	c	cc	
<i>Luria lurida</i> (Linnaeus, 1758)	+		
<i>Muricopsis cristata</i> (Brocchi, 1814)	+		
<i>Peltodoris atromaculata</i> Bergh, 1880	+		
Mollusca - Bivalvia			
<i>Arca noae</i> Linnaeus, 1758	+		
<i>Barbatia barbata</i> (Linnaeus, 1758)	+		
<i>Chama gryphoides</i> Linnaeus, 1758	+		
<i>Lithophaga lithophaga</i> (Linnaeus, 1758)	c	+	
<i>Musculus costulatus</i> (Risso, 1826)	+		
<i>Rocellaria dubia</i> (Pennant, 1777)	c	+	
<i>Spondylus gaederopus</i> Linnaeus, 1758	+		
Mollusca - Cephalopoda			
<i>Octopus vulgaris</i> Cuvier, 1797	+		
Annelida - Polychaeta			
<i>Eupolymnia nebulosa</i> (Montagu, 1818)	+		
<i>Protula</i> sp.	c	+	

(continued)

Table 2 (continued)

Taxa	front part of the cave	middle part of the cave	end part of the cave
<i>Serpula</i> sp.	c	+	
Serpulidae indet.		cc	c
Arthropoda - Crustacea			
<i>Galathea strigosa</i> (Linnaeus, 1761)	+		
<i>Hemimysis margalefi</i> Alcaraz, Riera & Gili, 1986	+	c	
<i>Homarus gammarus</i> (Linnaeus, 1758)	+		
<i>Palaemon serratus</i> (Pennant, 1777)	+	c	
<i>Palinurus elephas</i> (Fabricius, 1787)	+		
<i>Stenopus spinosus</i> Risso, 1827	+	+	
Bryozoa			
<i>Adeonella polystomella</i> (Reuss, 1848)	c		
<i>Crisia sigmoidea</i> Waters, 1916	+		
<i>Fron dipora verrucosa</i> (Lamouroux, 1821)	c		
<i>Margaretta cereoides</i> (Ellis & Solander, 1786)	c		
<i>Myriapora truncata</i> (Pallas, 1766)	c		
<i>Schizotheca serratimargo</i> (Hincks, 1886)	c		
<i>Scrupocellaria scrupea</i> Busk, 1852	c		
Brachiopoda			
<i>Joania cordata</i> (Risso, 1826)	+		
<i>Novocrania anomala</i> (Müller, 1776)		cc	
Echinodermata			
<i>Antedon mediterranea</i> (Lamarck, 1816)	+		
<i>Arbacia lixula</i> (Linnaeus, 1758)	+		
<i>Echinaster (Echinaster) sepositus</i> (Retzius, 1783)	+		
<i>Hacelia attenuata</i> Gray, 1840	+		
<i>Holothuria (Panningothuria) forskali</i> Delle Chiaje, 1823		+	
<i>Marthasterias glacialis</i> (Linnaeus, 1758)	+		
<i>Ophiaster ophidianus</i> (Lamarck, 1816)	+		
<i>Ophiothrix fragilis</i> (Abildgaard, in O.F. Müller, 1789)		+	
<i>Paracentrotus lividus</i> (Lamarck, 1816)	+		
Chordata - Ascidiacea			
<i>Halocynthia papillosa</i> (Linnaeus, 1767)	+	+	
Chordata - Actinopterygii			
<i>Apogon imberbis</i> (Linnaeus, 1758)	c	c	
<i>Chromis chromis</i> (Linnaeus, 1758)	+	+	
<i>Conger conger</i> (Linnaeus, 1758)	+		
<i>Diplodus vulgaris</i> (Geoffroy Saint-Hilaire, 1817)	+		
<i>Gobius cruentatus</i> Gmelin, 1789	+		
<i>Grammonus ater</i> (Risso, 1810)			+
<i>Mullus barbatus barbatus</i> Linnaeus, 1758	+		
<i>Oblada melanura</i> (Linnaeus, 1758)	+	+	
<i>Parablennius rouxi</i> (Cocco, 1833)	+		
<i>Phycis phycis</i> (Linnaeus, 1766)	+		
<i>Sciaena umbra</i> Linnaeus, 1758	+		
<i>Scorpaena notata</i> Rafinesque, 1810	+		
<i>Serranus scriba</i> (Linnaeus, 1758)	+		
<i>Spicara maena</i> (Linnaeus, 1758)	+		
<i>Thorogobius ephippiatus</i> (Lowe, 1839)	c	c	
Total no. of taxa:	122	42	20